Cooperative Behavior of Kinetically Constrained Lattice Gas Models of Glassy Dynamics

Cristina Toninelli,[1] **Giulio Biroli,**[2] **and Daniel S. Fisher**[3]

Kinetically constrained lattice models of glasses introduced by Kob and Andersen (KA) are analyzed. It is proved that only two behaviors are possible on hypercubic lattices: either ergodicity at all densities or trivial non-ergodicity, depending on the constraint parameter and the dimensionality. But in the ergodic cases, the dynamics is shown to be intrinsically cooperative at high densities giving rise to glassy dynamics as observed in simulations. The cooperativity is characterized by two length scales whose behavior controls finite-size effects: these are essential for interpreting simulations. In contrast to hypercubic lattices, on Bethe lattices KA models undergo a dynamical (jamming) phase transition at a critical density: this is characterized by diverging time and length scales and a discontinuous jump in the long-time limit of the density autocorrelation function. By analyzing generalized Bethe lattices (with loops) that interpolate between hypercubic lattices and standard Bethe lattices, the crossover between the dynamical transition that exists on these lattices and its absence in the hypercubic lattice limit is explored. Contact with earlier results are made via analysis of the related Fredrickson–Andersen models, followed by brief discussions of universality, of other approaches to glass transitions, and of some issues relevant for experiments.

KEY WORDS: Kinetically constrained lattice gases; glassy dynamics; ergodicity-breaking transition.

1. INTRODUCTION

The glass transition – whether a true transition or a sharp crossover in the dynamics – is one of the longest standing unsolved puzzles in condensed

[1]Laboratoire de Physique Théorique de l'ENS, 24 rue Lhomond 75231 Paris Cedex, France; e-mail: cristina.toninelli@lpt.ens.fr
[2]Service de Physique Théorique, CEA/Saclay-Orme des Merisiers, F-91191 Gif-sur-Yvette Cedex, France
[3]Lyman Laboratory of Physics, Harvard University, Cambridge, MA 02138, USA

matter physics. Many liquids, when cooled fast enough to avoid crystallization, initially remain liquid but at lower temperatures appear to freeze into solid-like structures that nevertheless show no signs of crystalline order. The time scales for structural relaxation in such metastable *super-cooled* regimes increase dramatically as the temperature is lowered and materials are conventionally called glasses when the structural relaxation times are longer than those accessible in typical experiments. In *fragile liquids* the relaxation time τ increases more rapidly than Arrhenius[1,2] and can be characterized by an effective activation free energy $d \log \tau / d(1/T)$ that increases by as much as a factor of twenty over a narrow temperature range.[2] Moreover, near glass "transitions", relaxation processes typically become complicated,[1] often characterized by stretched exponential decay of temporal correlations. Concomitantly, persistent spatial heterogeneities appear in both experiments[3,4] and numerical simulations.[5–8]

Yet, in spite of a great deal of theoretical effort over the past few decades, a real understanding of these and related phenomena is still lacking. Indeed, the most basic issues are still unresolved: Is the rapid slowing down due to proximity to an equilibrium phase transition of some kind (albeit perhaps in a restricted part of phase space)? Or is the underlying cause entirely dynamical? The latter scenario is supported by the lack of evidence for a diverging static correlation length and the weak temperature dependence of structural correlations,[2] while growing dynamical correlation lengths have been found in both experiments and simulations.[3,8] Whether or not there is an actual transition of some kind, what is the physical mechanism responsible for the slowing down of the dynamics and the growth of dynamical length scales?

Theoretical progress has been hampered by a shortage of models that capture at least some of the features believed to be essential, yet are simple enough to analyze. In other fields of statistical physics simple models have played vital roles leading to new understanding, to sharpening of questions, and to development of improved models.

1.1. Kinetically Constrained Lattice Models

One of the few types of simple models for glasses are the *kinetically constrained* models, in particular, lattice models with constrained dynamics; for reviews see. refs. 9, 10. In this paper, we focus on a particularly simple class of models introduced by Kob and Andersen (KA).[11] Before introducing these KA models and presenting our results, we give a short overview of kinetically constrained models more generally, including their motivation and the key questions about their behavior that could provide a deeper understanding of glass transitions in real systems.

The basic Ansatz that motivates kinetically constrained models (see e.g. ref. 12) is that the key to glass transitions is the geometrical constraints on rearrangements of the atoms or molecules and the effects of these constraints on the dynamics; static correlations, beyond those present in dense liquids, are assumed to play no role. The simplest models, which include KA models, are stochastic lattice gases with no static interactions beyond a hard core which restricts each site to be occupied by at most a single particle. The non-trivial aspect of these models arises from *local constraints* that are imposed on the motion of particles. Typically, the dynamics is given by a continuous time Markov process with each particle attempting, at a fixed rate, to jump to a randomly chosen empty neighboring site, but such a move is allowed only if the local configuration satisfies one or more constraints that depend on occupations of other nearby sites.

The motivation for the kinetic constraints in conservative models arises from the behavior of molecules in dense liquids: the presence of surrounding particles can severely inhibit the motion of a molecule. In particular, a molecule can be *caged* by its neighbors in such a way as to stop it moving a substantial distance until the cage is opened by the motion of other particles. When caging is ubiquitous, such local constraints can produce a degree of cooperative behavior that slows down the dynamics: one can readily imagine this to be the underlying mechanism that causes glass transitions. Since the idea behind the caging picture is that glass transitions are purely dynamical phenomena, with any changes in static correlations playing a minor role (see e.g. ref. 12), it is natural to explore models whose dynamics satisfy detailed balance with respect to some simple ensemble, in particular the trivial measure that is uniform over all configurations with the same number of particles: this corresponds to ignoring static interactions beyond hard cores. (These models are therefore quite different from the *statically* constrained "lattice glass models" introduced in ref. 13). Because of the neglect of interactions beyond hard cores, no equilibrium transition can take place in purely kinetically constrained models; clearly they cannot approximate the behavior of glass-forming liquids in all regimes, including the supercooling that avoids crystallization. Nevertheless, despite their simplicity and discrete character, kinetically constrained lattice models might still capture, at least on some range of time scales, the key dynamical aspects of real glass transitions. Indeed, numerical simulations show that some such models do display sluggish dynamics and much phenomenology that is reminiscent of glassy behavior and its onset as density increases.[9, 10] There has been a renewal of interest in these models for explaining the behavior of glass-forming liquids.[12, 14–25] Kinetically constrained lattice gases have also been studied in the context of granular systems[26] which also display a glass-like

dynamical arrest as their density is increased; this so-called *jamming transition*[27,28] occurs at a density well below close–packing density and can thus not have purely entropic origin.

Note that there is a similar class of kinetically constrained models whose elementary degrees of freedom are spins and not particles. An important example on which we will focus on Section 6 is provided by the Fredrickson and Andersen (FA) models.[29] These are the non-conservative version of the previous ones: there is no static interaction among spins on different sites and the non-trivial aspect arises from the local constraints imposed on the possible spin flips. In this case, the motivation for kinetic constraints comes from the concept of *dynamic facilitation*:[12,29] the evidence of dynamical heterogeneities, i.e. the existence of regions of space with very different relaxation times suggests that, on a coarse grained level, supercooled liquids might be considered as a mixture of mobile and non-mobile regions. The non-conservative character comes from the fact that the ratio of mobile to non-mobile regions is non-conserved in time. Kinetic constraints arise from the fact that the vicinity of mobile regions is required in order to enable (*facilitate*) mobility in a non-mobile regions.

1.2. Characterization of Possible Glass Transitions

The most crucial questions about kinetically constrained models of glasses are whether dynamical arrest takes place with increasing density, and, if so, whether this is the result of some type of sharp transition or instead a gradual freezing. In either case, one needs to understand the cooperative nature of the dynamics: in particular, the emergence of growing length scales that characterize the cooperativity.

We briefly sketch several possible scenarios for glass transitions. The most striking possibility would be an actual *ergodic/non-ergodic transition* at some critical density: this possibility, which corresponds to an analogous conjecture for the nature of the dynamical arrest in glass forming liquids, is the primary subject of the present paper. Because of the simple nature of the KA models, this question can be completely separated from possible changes in equilibrium static behavior. As mentioned above, for kinetically constrained models whose dynamics conserves the number of particles and satisfies detailed balance with respect to the uniform (non-interacting) measure, the trivial distribution that is flat over all configurations with the same density is always stationary and there can be no equilibrium transition. Nevertheless, due to the constraints on the allowed particle moves, ergodicity could be broken. Non-ergodicity means that, starting from an initial distribution which is not orthogonal with respect to the equilibrium measure, time averages of local quantities would *not*

converge to averages over the static equilibrium ensemble[30] even in the limit of long times. In other words, it corresponds to the existence of subsets of the configuration space which have non-zero measure (w.r.t. the equilibrium distribution) and in which the system can get trapped for infinite time. This certainly occurs for some kinetically constrained models on *finite* lattices for which the configuration space typically breaks into *disconnected irreducible components*: i.e. there exist two or more sets of configurations that can not be connected to one another by any sequence of allowed moves. A key question is whether this non-ergodicity can persist in the thermodynamic limit for which the grand canonical ensemble at fugacity ρ (Bernoulli product measure at density ρ) is an equilibrium distribution. Specifically, can an ergodic/non-ergodic transition occur at some density ρ_c such that the dynamics on the infinite lattice is ergodic for $\rho < \rho_c$, but not ergodic for $\rho > \rho_c$? Such an ergodicity-breaking transition is often considered an *ideal glass transition*; it has been advocated as the primary cause of the slowing down of glass-forming liquids. Ergodicity-breaking transitions have been found to occur in several approximate theories, including in mode coupling theory[31] and in fully connected quenched random spin models.[32]

A weaker type of dynamical arrest could in principle take place even if ergodicity is not broken: in particular, a *diffusive/sub-diffusive transition* of the dynamics. Indeed, the motion of a *tracer particle* could become non-diffusive at high densities: this could be observed by singling out of an infinite system that is in equilibrium, one particle, the tracer, and following its motion. There exists a general rigorous result that restricts the behavior: as long as the dynamics is ergodic, the position of a tagged particle converges under diffusive space-time rescaling to Brownian motion with a density-dependent self-diffusion coefficient $D_S(\rho) \geqslant 0$.[33,34] But in order for the tagged particle to diffuse, the self-diffusion coefficient has to be nonzero: for the normal hard core lattice gas (simple symmetric exclusion) in $d > 1$, this has been proven[33] and in ref. 35 the result has been extended to all the models such that the rate of any given jump to an empty neighbor is bounded away from zero. For kinetically constrained lattice gases, however, the tagged particle *could* be slowed enough that D_S becomes zero at sufficiently high density. A diffusive/sub–diffusive transition would then presumably take place at some critical density, ρ_D with $D_S > 0$ for $\rho < \rho_D$ but $D_S = 0$ for $\rho > \rho_D$. Such a transition has been conjectured to occur in real glasses: and several experiments on supercooled liquids near their glass transition indeed show a striking decrease of the mean square displacement of a tracer particle over the observed range of times.[2]

Another way in which diffusion could potentially break down involves the breakdown of the conventional hydrodynamical limit that usually

holds on long length and time scales.[34] For lattice gases (and more generally for systems with particle number conservation but no momentum conservation) the coarse-grained density profile evolves, at long times, via the diffusion equation, $\partial_t \rho = \nabla (D(\rho)\nabla\rho)$, with the diffusivity, $D(\rho)$, dependent on the local density. For generic kinetically constrained stochastic models, proving the existence of the hydrodynamic limit, as has been done for conventional hard core models, is not a trivial task. The natural conjecture, if a transition of some kind did occur, would be the vanishing of the macroscopic diffusivity, $D(\rho)$, at high densities. This would give rise to a form of *macroscopic arrest*, in which density profiles at high densities would evolve, if at all, only sub-diffusively. Note that, in contrast to the diffusion of a tagged particle, evolution of density profiles need not involve motion of individual particles far from their initial neighbors: density diffusion and self-diffusion thus probe rather different aspects of the dynamics.

Consideration of the types of macroscopic diffusion raises the more general question of relaxation towards equilibrium: this could be anomalously slow even if the system remains ergodic at all densities. An interesting quantity to consider is the dynamical structure factor, the Fourier transform of the density–density correlation function at non-zero wave vector. For normal lattice gases, the dynamical structure factor decays exponentially at long times but for kinetically constrained models, the relaxation could perhaps be slower than exponential, at least above some critical density. Indeed in numerical simulations of some kinetically constrained models at high density, sub-exponential relaxation has been found over a range of more than three decades.[11] This, as well as the relaxation of different response functions (see e.g. refs. 14, 36) is usually fitted with a *stretched exponential* $S(t) \sim \exp[-(t/\tau)^\beta]$, with $\beta < 1$ (also called a Kohlrausch–Williams–Watts function). Many glass-forming liquids show similar behavior with relaxation functions well-fitted by simple exponentials at high temperatures, but by stretched exponentials at low temperatures.[2, 37, 38] In glass-forming liquids this behavior arises from the superposition of many relaxations with different decay rates, each corresponding to different spatial regions within a dynamically heterogeneous spatial structure which persists for longer time scales.[3] If such sub-exponential relaxation does occur in kinetically constrained models – even if only over a limited range of times – a detailed understanding of it would shed light on the behavior of more realistic systems.[4]

---

[4]It is important to note that stretched exponential relaxation can occur in the absence of such complications as heterogeneities: indeed, the two dimensional Ising model with non-spin-conserving dynamics exhibits just such behavior in its ordered phase.[39]

Numerical simulations of Kob-Andersen models, as reviewed below, have found very sluggish dynamics at high density,[11] with much phenomenology that is very similar to glass-forming liquids. Is this a signature of some type of real dynamical glass transition at a critical density? More generally, does one exists for at least some versions of the KA models? If not, what is the basic mechanism for the extremely rapid onset of the slowing down as the density is increased? Are there collective processes involved? What if any, are the characteristic length scales, and how are the time scales related to these? What is the physical mechanism giving rise to the dynamical heterogeneities? And, most importantly, what can one learn from the KA models about the behavior of more realistic models? In this paper we will address all of these, although the last, regrettably, only to a limited extent.

Some of the results of this paper have already been presented in a short letter[37] and the proof of the positivity of the self-diffusion coefficient for KA models was presented in ref. 41; these both made use of the results derived in the present paper.

1.3. KA Models: Definition and Heuristics

Kob–Andersen models were introduced,[11] as mentioned above, to test the conjecture that *cage effects* in liquids can induce a sudden onset of dynamical arrest as the density increases thereby being responsible for a glass transition in such systems. The conditions for particles to be able to move in KA models mimic those caused by the geometrical constraints imposed by surrounding particles on the motion of molecules in dense liquids.

The Kob–Andersen models we consider are natural generalizations to higher dimensions of those of ref. 11 (the original model corresponds to the choice $d=3, m=3$ in our notation): they are defined on d-dimensional hypercubic lattices $\Lambda \in \mathbb{Z}^d$ with zero or one particles allowed per lattice site and a parameter, m, that represents the set of allowed particle motions as explained below (for a more formal definition see Section 2.5). Each particle *attempts*, at rate unity, to move to a randomly chosen one of its $z=2d$ nearest neighbor sites. But a move from a site x to a neighboring site y is allowed *only if* site y is empty *and* the particle has no more than m occupied neighbors both before and after the move. If any of these constraints is not satisfied the particle remains at site x (at least until its next attempt to move). The possible values of m range from $m=0,\ldots,2d-1$, the upper limit being one less than the coordination number, z (due to the hard core constraint). In the following we will always focus on the grand canonical ensemble, therefore the control parameter will be the particle density, ρ.

As the interesting behavior occurs at high densities it is useful to reformulate the rules in terms of *vacancy* motion, i.e dynamics of the empty sites. As can readily be verified, the above constraints with parameter m correspond to *vacancies* allowed to move *only if* both the initial site before the move, *and* the final site after the move, have *at least* $s = z - m - 1$ *neighboring vacancies*. The hypercubic KA models are thus completely defined by the parameters d and m, or equivalently, d and s; we will usually use the latter. The special case $m = 2d - 1$ corresponds to $s = 0$: this KA model thus corresponds exactly to conventional hard-core lattice gas dynamics (i.e. simple symmetric exclusion process).

For all values of s the *equilibrium static properties* are identical to those of the hard-core lattice gas model with no other interactions, and are hence *trivial*. But the dynamics depends radically on s. For $s \geqslant d$, the dynamics is so constrained that KA models are trivially non-ergodic at any $\rho \in (0, 1]$. This can be checked by noticing that a fully occupied hypercube of particles of any size can never be broken up, therefore at any finite density there exists a finite fraction of particles which are forever blocked. We thus focus on $0 < s < d$.

Why might one expect interesting dynamics for $s \geqslant 1$? In contrast to the conventional lattice gas ($s = 0$) for which individual vacancies can move freely, for non-zero s on hypercubic lattices, there are *no finite mobile clusters of vacancies* that can move freely – albeit together – in an otherwise fully occupied system. By this we mean that, if the surrounding lattice is completely filled, it is not possible to construct a path of allowed nearest neighbor moves through which one can shift the cluster of vacancies. This follows from the existence of infinite frozen configurations which, as none of the particles in them can move at all, impede the motion of any cluster of vacancies. The simplest infinite frozen configuration is a fully occupied slab of particles that is infinite in $d - s$ of the lattice directions and has width two in the other s directions: by construction, none of the particles in such a slab can move with the KA dynamical rules with parameter s. (In contrast to the absence of mobile clusters of vacancies on hypercubic lattices with non-zero s, on a two-dimensional triangular lattice with $s = 1$, isolated vacancies cannot move but neighboring pairs of vacancies can move freely and equilibrate the system (see ref. 41 for a detailed and rigorous discussion).)

Although for non-zero s on hypercubic lattices there are no finite mobile clusters of vacancies, neither are there finite frozen clusters for $s < d$. This follows because a particle at a corner of any fully occupied region that is surrounded by empty sites can move; thus on an infinite lattice there are *no finite frozen clusters*. Nevertheless, there do exist *infinite frozen sets* of particles such as the completely filled slab defined above.

Such simple frozen configurations have very little entropy – in fact, zero entropy density – but a much larger set of frozen configurations exist that *does* have non-zero entropy density. For example, for the simplest case, $s = 1$ on a square lattice, in addition to configurations with a single two-wide frozen slab that is infinitely long, any configuration with a set of such slabs that each begin and end at T-junctions with other such slabs will be frozen. A crucial question about static configurations is thus whether, at sufficiently high densities, almost all infinite configurations contain an infinite – and hence connected – set of frozen particles. As we shall see, answering this is by no means trivial. For all the non-trivial cases, the above observations imply that the sluggish dynamics at high densities must be *intrinsically collective*, involving rearrangements of increasingly larger and larger regions as the density increases.

1.4. Previous Numerical Results

Before introducing the analytic methods we will use, we briefly summarize the results of various numerical simulations of the best studied KA model: the three – dimensional case with $s = 2$. It has been suggested that these simulations provide support for the conjecture of an ergodic/non-ergodic transition at a non-trivial density, $\bar{\rho}$. In ref. 11 the self-diffusion coefficient of a tagged-particle was measured and the results found to fit well a power law form that vanished at a finite density: $D_s \propto (\rho - \bar{\rho})^{\alpha}$ with $\alpha \simeq 3.1$ and $\bar{\rho} \simeq 0.881$. Approaching this same *apparent critical density* the rate of temporal relaxation of density-density correlations appeared to vanish as an inverse power of $\rho - \bar{\rho}$. Both results – which hold over roughly four decades of D_S and two decades of $\rho - \bar{\rho}$ – were strongly suggestive of a dynamical glass transition at $\rho = \bar{\rho}$.

Furthermore, the asymptotic decay of the Fourier transform of density–density correlation function was fitted with the form $S(t) \simeq \exp[(-t/\tau)^{\beta}]$ with an exponent β close to one (exponential decay) for low and intermediate densities and decreasing monotonically with ρ (stretched exponential decay) at sufficiently high density (for $\rho > 0.75$).

Later work found that other typical features of "glassy dynamics" occur at high densities in this $d = 3$, $s = 2$ model.

In ref. 20 numerical simulations found *dynamical heterogeneities* to be persistent for very long times, at densities higher than roughly $\bar{\rho}$. In ref. 21 the effects of boundary sources of particle – corresponding to a grand canonical ensemble – were studied, in particular by quenching the chemical potential μ of the sources below the apparent critical value that corresponds to the equilibrium $\mu(\bar{\rho})$. A non-equilibrium regime was

evident, and "aging" effects similar to those observed in glasses were found. Properties that play roles in various theoretical approaches to glass transitions have also been studied. In particular, the relationship between the "configurational entropy" of the number of distinct frozen configurations and an "effective temperature" which emerges from the aging dynamics was investigated to test Edward's hypothesis[22] as formulated by Kurchan in the context of aging dynamics; this had been found in certain mean field models studied in the context of glasses, see ref. 23. Edwards' hypothesis appears consistent with numerical results on the $d=3, s=2$ KA model.[22]

The results announced in ref. 40 and explained in detail in the following provide a theoretical framework to interpret numerical simulations. Two recent works[14,24] have indeed analyzed the $d=3$, $s=2$ KA model taking into account our results and checking some of our analytic predictions.

1.5. Summary of Exact Results

From the numerical simulations described above, it is clear that the dynamics of some KA models is very sluggish at high density and displays much of the basic phenomenology of glassy dynamics observed in many experimental systems. Furthermore, there appears to be a rather sharp onset of the glassy behavior as the density is increased. The analytical methods of this paper yield an understanding of the mechanisms underlying the slow dynamics of KA models and address the basic qualitative and quantitative questions about them.

The primary question is whether there exists some kind of *actual* dynamical transition for the $d=3$ $s=2$ (or other) KA model, or whether the *apparent* "transition" seen in simulations is only a result of the finite size and finite time limitations of such simulations. We first investigate whether an ergodic/non-ergodic transition can occur at a non-trivial density in KA models. We conclude that, for any dimension and any choice of the constraint parameter $s < d$, an *ergodic/non-ergodic transition cannot take place* at a non-trivial density $\rho \in (0, 1)$. In other words, the sluggish behavior found in simulations cannot be the mark of an "ideal" glass transition. More quantitatively, we derive a density dependent characteristic length scale $\Xi(\rho)$ which separates two different regimes: for samples with linear dimensions $L \ll \Xi(\rho)$ the configuration space breaks into many ergodic components; while for those with $L \gg \Xi(\rho)$ a single ergodic component dominates – although other disconnected components still exist (a precise definition of $\Xi(\rho)$ is given below). The length, Ξ, whose dependence on ρ varies with d and s, diverges at high density: $\Xi(\rho) \sim \exp\exp(c/(1-\rho))$ for the $d=3$ and $s=2$ model. Therefore, large systems

of size L^3, are likely to appear ergodic only if $\rho < \rho_c(L) = 1 - (c/\log\log L)$. Although for smaller sizes the apparent ergodicity breaking takes place at lower values of the density, the dependence on L is very weak for large L. Of course, to properly analyze data from simulations, knowledge of the *existence* of a cross over length is a key ingredient for disentangling the finite size effects which will always be limiting at high densities.

The fact that ergodicity holds in infinite systems at all densities for $s < d$, does not rule out the possibility of a more subtle type of dynamic transition at a non-trivial density. In particular, a diffusive/sub-diffusive transition, if it existed, would explain the apparent vanishing of the self-diffusion coefficient found in the above-mentioned numerical simulations.[11] We have studied the asymptotic behavior of the diffusion coefficient, D_S, of a tagged particle. The result, discussed in detail in ref. 40, 41, is that D_S is strictly positive at any density $\rho < 1$, so that *a diffusive/subdiffusive transition cannot take place*. Moreover, this analysis[40] unveils the nature of the collective processes which are needed for both equilibration and diffusion at high density. The characteristic time scale, τ, of the slow cooperative dynamics can be calculated and for the non-trivial cases, namely $s < d$, τ diverges faster than any inverse power of $1 - \rho$ as $\rho \to 1$.

Given these results for general KA models on hypercubic lattices, an immediate question arises as to whether KA models can *ever* exhibit a transition at a non-trivial density: if this can occur, it raises the possibility that the surprisingly sharp onset of the slow dynamics observed in simulations in, for example, $s = 2$, $d = 3$, might be due to the "ghost" of such a transition. Experience suggests that the most likely models in which to find actual transitions are "mean-field-like" models;[32] thus we study KA models on tree structures, more precisely, Bethe lattices, which often provide realizations of mean field approximations. We find that on Bethe lattices *there exists a critical density*, ρ_c, above which ergodicity is broken and phase space breaks up into many disconnected components. The transition at ρ_c has aspects of both first order and second order transitions.

An interesting question that we leave open for future investigation is the hydrodynamic behavior of KA models on hypercubic lattices. Although we conjecture that on large enough length and time scales hydrodynamics will be valid at any density less than one for ergodic KA models, this might be very hard to prove. Assuming that the conjecture is correct, an important issue, related to both experiments[42] and simulations[8] of glass-forming liquids, is the characteristic length and time scale beyond which hydrodynamic behavior sets in, in particular, how these scales increase with density.

A recent interesting analysis of this behavior within Kinetically Constrained models have been presented in ref. 25.

1.6. Outline

The organization of the remainder of this paper is as follows: In Section 2 we analyze $s < d$ KA models on hypercubic lattices and prove ergodicity for any density $\rho < 1$. First, in 2.1 we analyze the simplest interesting case, $d = 2$, $s = 1$, and prove that with unit probability there exists an irreducible component of the configuration space in the thermodynamic limit and find an upper bound, $\Xi^u(\rho)$, on the crossover length $\Xi(\rho)$. In 2.2, we extend these results to the case $d = 3$, $s = 2$ originally considered by KA and in 2.3 derive analogous results for $s = 1$ in general d. The convergence of large systems to the infinite system behavior is studied in 2.1.4; we prove that for $L > \Xi^u(\rho)$ the probability of the maximal irreducible component goes to one at least exponentially rapidly. Using these results, in 2.4 we extend the irreducibility proof and find upper bounds for the crossover length for all $s < d$. Finally, in 2.5 we prove that irreducibility of the configuration space implies ergodicity.

Section 3 is devoted to quantitative results on the cross-over lengths. In 3.1, by using recent bootstrap percolation results to obtain lower bounds on $\Xi(\rho)$ and combining these with the upper bounds, we find the asymptotic behavior of the density-dependence of the cross over length, up to an undetermined constant. In Section 3.2, we calculate the exact value of this constant for the case $d = 2$ $s = 1$ via the identification of the dominant mechanism which restores ergodicity in large systems at high density. In 3.3 we formulate an analogous conjecture for the dominant high density behavior of the original KA model, $d = 3$ $s = 2$.

In Section 4 the physical picture for the cooperative high density dynamics (which was presented in ref. 40) is explained and related to the results derived in this paper; details are left for a forthcoming paper.

In Section 5 KA models on Bethe lattices are studied. After recalling (Section 5.1) the definition and some properties of Bethe lattices, in 5.2 and 5.3 recursive relations are derived whose fixed point solution implies that an ergodicity-breaking transition takes place at a non-trivial critical density ρ_c, for any $s < k$ — the branching parameter of the Bethe lattice. The transition is shown to be discontinuous for $s < k - 1$ (Section 5.3.1) but continuous for $s = k - 1$ (Section 5.3.2). The existence and location of this transition are related to a boostrap percolation transition in 5.3.3. In Section 5.4, the focus is on quantitative results for Bethe lattice models: we analyze in some detail the character of the transition in the cases $k = 3$, $s = 1$ and $k = 5$, $s = 3$ and present results of numerical simulations for the $k = 3$, $s = 1$ model. The behavior of the density–density correlation function and the corresponding susceptibility are studied, along with the configurational entropy, $S_c(\rho)$. By establishing a lower bound we prove that

$S_c(\rho)$ jumps to a non-zero value at ρ_c. We end this section, in 5.5, by extending to KA model on decorated Bethe lattices: graphs with finite size loops that interpolate between simple Bethe lattice and finite-dimensional hypercubic lattices.

In Section 6 we analyze the related FA models, proving, in 6.2, ergodicity at any finite temperature (completing an almost complete proof that had been given by FA themselves). In 6.3 we give quantitative predictions on length and time scales for the $d = 2$ two spin facilitated FA model.

Finally, in 7, we draw conclusions and discuss some possible connections of our results to other theoretical treatments of glass transitions. In particular, the analogy of KA models on Bethe lattices to fully connected random p-spin models. We also comment briefly on possible extensions of KA models and connections to experiments.

2. RIGOROUS RESULTS FOR KA MODELS ON HYPERCUBIC-LATTICES

In this section we analyze KA models on hypercubic lattices with the parameter s in the non-trivial range $1 \leqslant s \leqslant d - 1$. We prove that for any density $\rho < 1$, on an infinite lattice such KA models are *ergodic*. In contrast, as explained earlier, for larger values of s, $s \geqslant d$, KA models on hypercubic lattices are non-ergodic for all positive ρ because of the existence of finite frozen clusters. There are thus only two possible behaviors for hypercubic lattices: either the KA process in the thermodynamic limit is ergodic at any density, i.e. $\rho_c = 1$, or else it is never ergodic, i.e. $\rho_c = 0$; therefore *ergodic/non-ergodic transitions cannot take place in KA models on hypercubic lattices* for any d and s.

The strategy of the proof is as follows. Let $\Lambda \in \mathbb{Z}^d$ be an hypercube of linear size L. First we identify a component of the configuration space $\Omega_\Lambda \equiv \{0, 1\}^{|\Lambda|}$ and show that it is *irreducible*, i.e. any two different configurations belonging to this component can be connected to each other by a sequence of elementary moves allowed by the KA rules. Second, we prove that, with respect to the natural measure on the space of configurations, Bernoulli product measure $\mu_{\Lambda,\rho}$, the *probability of this single irreducible component goes to unity for $L \to \infty$*. Finally we prove that, thanks to the product form of Bernoulli measure, the *existence of an irreducible component with unit probability implies ergodicity for the infinite system*, $\Lambda = \mathbb{Z}^d$.

In the first four subsections, we give the first and second steps of the proof for all choices of d and s, leaving to 2.5 the last step, which is proved by a general argument that is independent of the specific parameters.

We start with the simplest non-trivial model, $d = 2$, $s = 1$, giving the most details for this case.

2.1. Irreducibility for *d* = 2, *s* = 1

The only non-trivial model on a square lattice is the case $s = 1$: vacancies can move if and only if they have a neighboring vacancy both before and after the move.

2.1.1. Frameable Configurations

In order to construct the large irreducible component of configuration space we start by defining a subset of the configurations in it. Specifically, let us define *framed* configurations of any square or rectangle as those in which all the boundary sites are empty (see Fig. 1). We then define as *frameable* any configuration from which, by an allowed sequence of elementary moves, a *framed* configuration can be reached. As we show below, any two framed configurations that have the same number of particles can be connected to one another by a sequence allowed moves; the same then applies to all frameable configurations by definition.

2.1.2. Irreducibility of Frameable Set

The irreducibility of a set of frameable configurations can be checked as follows. Note that even though it is not needed for the present purposes we shall prove irreducibility considering the particles as distinguishable. This result is important for the proof of the positivity of the self-diffusion coefficient.[41] Consider a pair of neighboring sites $\{i, j\}$, with for example particles A and B respectively on $\{i, j\}$ and j immediately to the right of i. To prove the needed result, it is enough to show that, for any choice of the framed configuration, it is possible to perform the permutation of
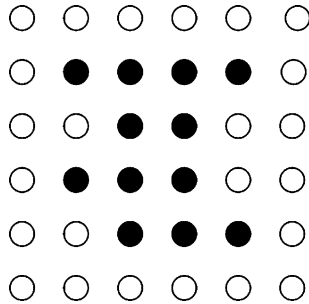

Fig. 1. A 6 × 6 framed configuration. Filled dots are occupied sites; empty dots vacant sites.
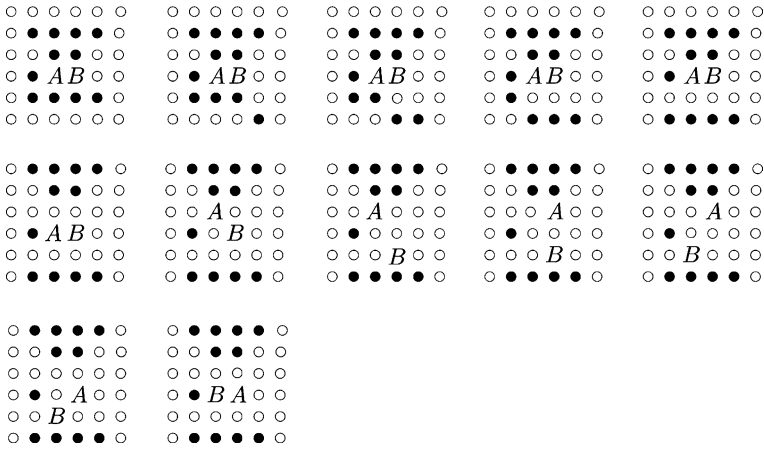
Fig. 2. Sequence of allowed elementary moves starting from a generic 6×6 framed configuration, whose net result is the exchange of two neighboring particles, A and B, inside the square. Figures in the first line show the elementary moves connecting the initial configuration to a configuration with the bottom row of holes raised by one. By analogous moves (skipped in the figure) one can lower the top row of holes of two steps. Now (first figure of second row) particles A and B are "sandwiched" between two rows of holes. The remaining figures show how to exchange particles A and B starting from this configuration. Note that no other particles have been moved during this exchange. The configuration which is equal to the initial one (first line, first figure) on the sites not occupied by A and B can subsequently be restored by using sequences of moves analogous to those in the first line to raise the one full row of holes and lower the other one.

A with B leaving at the end of the process all the other particles in their initial configuration.

Starting from the bottom right corner it is possible to raise the bottom row of holes as shown in first line of Fig. 2, and likewise starting from the top right corner, to lower the top row of holes. This procedure can be iterated until the row that contains sites i and j is "sandwiched" between two rows of holes (first configuration on second line of Fig. 2). At this point, using the surrounding vacancies, one can easily construct a path performing the desired permutation of particle A and B from site i to j (second and third line of Fig. 2). Following this exchange, the initial configuration of the rest of the lattice can be restored by reversing the moves of the two rows of holes after which all particles other than A and B have returned to their original sites. The full procedure can be performed if instead there is a particle and a hole on $\{i, j\}$. Since any framed configuration can be transformed to any other framed configuration with the same number of particles through a sequence of permutations of nearest neighbor particles and/or holes, all the framed configurations with the

same number of particles belong to the same irreducible component. By definition, so also do all frameable configurations, a much larger set.

2.1.3. Frameable Probability

The next step is proving that, of all configurations with density ρ, the fraction that are frameable, $\mu_{\Lambda,\rho}(\mathcal{F})$, approaches one in the limit $L \to \infty$. We will do this by first constructing a large subset of $\mathcal{F}$.

Consider a 4×4 configuration which has at its center a 2×2 square of holes – a 2×2 framed configuration –and in the surrounding shell at least two holes adjacent to each side of the inner square. It is easy to check (see Fig. 3) that such a 4×4 configuration is frameable. This procedure can be iterated to grow an $L \times L$ frameable configuration starting from a 2×2 nucleus of vacancies and requiring at least two vacancies in each side of each subsequent shell. Therefore, $\mu_{\Lambda,\rho}(\mathcal{F})$ is bounded from below by the probability, $\mu_{\Lambda,\rho}(\mathcal{F}^0)$, of frameable configurations constructed with this procedure from a 2×2 nucleus of vacancies centered at the origin (Fig. 4):

$$\mu_{\Lambda,\rho}(\mathcal{F}) \geqslant \mu_{\Lambda,\rho}(\mathcal{F}^0) = (1-\rho)^4 \prod_{l=1}^{(L-2)/2} (1 - \rho^{2l} - 2l\rho^{2l-1}(1-\rho))^4. \quad (1)$$

Note the as the size of the shell grows, the probability that there are the requisite number of vacancies on each side increases until becoming close to unity for sufficiently large shells: specifically when $l \gg 1/(1-\rho)$. The large L behavior of $\log\left(\mu_{\Lambda,\rho}(\mathcal{F}^0)\right)$ is determined by

$$4\log(1-\rho) + 4 \sum_l \log[1 - \rho^{2l} - 2l\rho^{2l-1}(1-\rho)]$$

$$\simeq 4\log(1-\rho) - 4 \sum_l [\rho^{2l} + 2l\rho^{2l-1}(1-\rho)], \quad (2)$$

which is a converging series for any $\rho < 1$. Therefore $\mu_{\Lambda,\rho}(\mathcal{F}^0)$ converges to a non-zero limit when $L \to \infty$ at fixed density.

Because of the divergence of the above series for $\rho = 1$, additional care is required to analyze the behavior when both $\rho \to 1$ and $L \to \infty$.
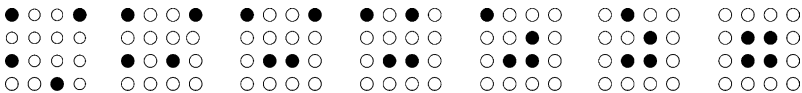

Fig. 3. Growing 4×4 frameable configurations from a 2×2 framed configuration.
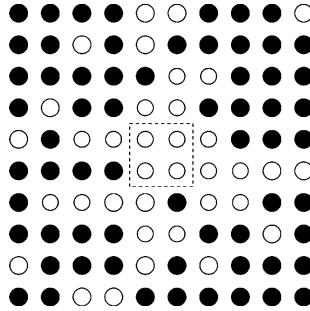
Fig. 4. An 8×8 frameable configuration obtained from the growing procedure. The dashed square indicates the position of the 2×2 seed. Note that the density in such configurations is small near the seed but higher farther away.

Let $a(\ell) \equiv \log(1 - \rho^{2\ell} - 2\ell\rho^{2\ell-1}(1-\rho))$. Since $a(\ell)$ is increasing in ℓ, the following inequality holds:

$$4a(1) + 4\int_1^{\frac{L-2}{2}} d\ell\, a(\ell) \leqslant \log \mu_{\Lambda,\rho}(\mathcal{F}^0) - 4\log(1-\rho)$$

$$\leqslant 4\int_2^{\frac{L-2}{2}+1} d\ell\, a(\ell), \tag{3}$$

where the last term can be rewritten by using the change of variables $y = \rho^{2\ell}$ and expanding for $\rho \simeq 1$ as

$$\lim_{L\to\infty}\int_2^{\frac{L}{2}} d\ell\, a(\ell) \simeq \frac{1}{2(1-\rho)}\int_0^1 dy\, \frac{\log(1 - y + y\log y)}{y}. \tag{4}$$

Therefore, by combining Eq. (3) and (4) and using $\lim_{\rho\to1}(1-\rho)\log(1-\rho) = 0$ we get

$$\lim_{\rho\to1}\lim_{L\to\infty}(1-\rho)\log\mu_{\Lambda,\rho}(\mathcal{F}^0) = 2\int_0^1 dy\, \frac{\log(1 - y + y\log y)}{y} \tag{5}$$

i.e., in the high density limit.[5]

$$\lim_{L\to\infty}\mu_{\Lambda,\rho}(\mathcal{F}^0) \equiv \mu_{\infty,\rho}(\mathcal{F}^0) \simeq e^{-\left(\frac{2c}{1-\rho}\right)} \tag{6}$$

[5]Note that here and in the following we will use for simplicity the loose notation $\mu_{\infty,\rho}(\mathcal{F}^0) \simeq e^{-\left(\frac{2c}{1-\rho}\right)}$ although the correct mathematical expression is $\log\mu_{\infty,\rho}(\mathcal{F}^0) \simeq -\left(\frac{2c}{1-\rho}\right)$ up to vanishing corrections in the $\rho \to 1$ limit.

with

$$c = -\int_0^1 dy \, \frac{\log(1 - y + y \log y)}{y}. \tag{7}$$

Moreover from

$$\log \mu_{\infty,\rho}(\mathcal{F}^0) - \log \mu_{\Lambda,\rho}(\mathcal{F}^0) \simeq \frac{2}{1-\rho} \int_1^{\rho^L} dy \, \frac{\log(1 - y + y \log y)}{y}$$

$$\simeq \frac{2}{1-\rho} \int_1^{\rho^L} dy(-1 + \log y)$$

$$= \frac{2}{1-\rho} \left(\rho^L \log[\rho^L] - 2\rho^L \right)$$

$$\simeq \frac{-4\rho^L}{1-\rho} \tag{8}$$

we find that $\mu_{\Lambda,\rho}(\mathcal{F}^0) \simeq \mu_{\infty,\rho}(\mathcal{F}^0)$ for $L \gg \xi_{2,1}(\rho)$, defining a characteristic length, $\xi_{d,s}(\rho)$, with

$$\xi_{2,1} = -\log(1 - \rho)/(1 - \rho), \tag{9}$$

which will play an important role in what follows.

We now need to get from the probability, $\mu_{\Lambda,\rho}(\mathcal{F}^0)$, of a frameable region centered at the origin, to the needed result: the probability that a square of size L is frameable about *some* center, $\mu_{\Lambda,\rho}(\mathcal{F})$, converges to unity for $L \to \infty$. To do this one must consider all the possible positions for the initial nucleus used in the growing procedure.[6] Naively, we could simply make the argument that in a very large system, it is extremely unlikely that the system would not be frameable around at least one of the many possible nuclei. But additional work is required to turn this argument into a proof since the events that the whole square is frameable starting from different nuclei are not independent. We postpone the actual proof to the end of Section 2.3, where we consider the generic d-dimensional case, and here just outline the argument.

The key idea is the following: from the above definition of ξ, the conditions needed to *further* expand a frameable square of size $L \gg \xi$ are satisfied with probability close to one. Therefore, whether or not one can grow frameable configurations starting from nuclei at the centers of *distinct* squares of

---

[6]The results obtained hold for the KA model on a finite square lattice with periodic boundary conditions. In this geometry, any point can be taken as the origin of the growing procedure.

size ξ are almost independent. By considering that there are $O\left(L^2/\xi^2\right)$ disjoint squares of size ξ inside the $L \times L$ square, Λ, we conclude that $\mu_{\Lambda,\rho}(\mathcal{F})$ is almost one for $L \gg \xi/\sqrt{\mu_{\infty,\rho}(\mathcal{F}^0)} \simeq \exp\left[c/(1-\rho)\right]$ and approaches one as $L \to \infty$. The rigorous version of this argument given in 2.3 completes the proof of irreducibility in the thermodynamic limit.[7]

Let us now turn to the analysis of finite size effects. As stated above, the probability of the irreducible frameable component goes to one when $L \to \infty$ at any fixed density $\rho \in [0, 1)$. On the other hand, for any finite and fixed value of L, the probability of any irreducible component is strictly smaller than one: blocked configurations exist and therefore the configuration space is never covered by a single component. Furthermore, when $\rho \to 1$ the probability $\mu_{\Lambda,\rho}(\mathcal{M})$ of the maximal irreducible component (the irreducible component with the highest probability) goes to zero since blocked configurations are more and more important and each one is in a different irreducible component. Therefore $\lim_{\rho \to 1} \mu_{\Lambda,\rho}(\mathcal{M}) = 0$ at fixed lattice size while $\lim_{L \to \infty} \mu_{\Lambda,\rho}(\mathcal{M}) = 1$ at fixed density. Thus the simultaneous $L \to \infty$ and $\rho \to 1$ limit depends on the relationship between L and ρ as the limit is taken: this is typical of finite-size behavior near phase transitions. The crossover length $\Xi_{2,1}(\rho)$ is defined to separate the "large" and "small" system behaviors so that by sending $L \to \infty$ and $\rho \to 1$ with $L \gg \Xi_{2,1}(\rho)$ or $L \ll \Xi_{2,1}(\rho)$, respectively, one obtains $\mu_{\Lambda,\rho}(\mathcal{M}) \to 1$ or $\mu_{\Lambda,\rho}(\mathcal{M}) \to 0$, respectively. This defines the limiting behavior of $\Xi(\rho)$ up to an overall constant factor. A more precise definition is possible, for example, by the sequence of (L, ρ) pairs for which $\mu_{\Lambda,\rho}(\mathcal{M}) = \frac{1}{2}$. Above results on the probability of the frameable component establish therefore an upper bound on the crossover length:

$$\Xi_{2,1}(\rho) \leqslant \Xi_{2,1}^u(\rho) \approx \exp\left[\frac{c}{(1-\rho)}\right], \tag{10}$$

with c defined in (7). The reason why Ξ^u is only an upper bound for the cross over length is because while our framing argument guarantees that for $L > \Xi^u$ a single irreducible component (the frameable one) dominates, it says nothing about the probability of the *maximal* irreducible component, which could already be close to unity for much smaller sizes. Indeed, if we have not got roughly the correct size-dependent conditions for frameability, $L \times L$ squares could be almost ergodic even for $(1-\rho)\log L \ll$

---

[7]In infinite volume the desired result $\mu_{\infty,\rho}(\mathcal{F}) = 1$ can be derived immediately from the above established $\mu_{\infty,\rho}(\mathcal{F}^0) > 0$ using ergodicity of Bernoulli measure. The more involved argument developed in Section 2.3 gives in addition the velocity of convergence to unity of the frameable probability. It is therefore needed to find a lower bound on the crossover length.

$(1 - \rho) \log \ \Xi^u$. This possibility is ruled out in Section 3.1 by establishing a lower bound Ξ^l that has similar density dependence to Ξ^u, ensuring that we do indeed have the correct asymptotic form, albeit with the wrong coefficient c. The exact coefficient will be calculated in Section 3.2 thanks to the definition of a different framing procedure.

The cross-over length, Ξ, is also the scale above which frozen sets of particles are unlikely to exist. In particular, a spanning network of fully occupied two-wide slabs that all start and end either at system boundaries or at T-junctions with other slabs – a frozen configuration–is likely to exist for squares of size $L < \Xi$, but unlikely to exist for much larger squares. How does this occur? In particular, if a number of squares of size somewhat smaller than Ξ are put together to make one of size a few times Ξ, what happens to the (formerly) frozen bars that terminated inside one of the original squares? A crucial feature is the *fragility* of a typical frozen network of slabs: if one slab is cut, as will occur if it ends on an edge of one of the now-interior smaller squares, this can trigger a catastrophic failure of most of the network. Such extreme fragility is why the set of all frozen configurations has measure zero in infinite systems in spite of its non-zero entropy density.

Before moving on to more complicated KA models, it is important to note that the whole proof of irreducibility is based on two ingredients: all configurations that contain a special frame of holes belong to the same irreducible component; and the frame can be created by starting from a small nucleus of vacancies and expanding to larger sizes by satisfying at each step requirements that becomes less and less severe probabilistically. Therefore, the basic result for the simple square lattice model we have considered thus far is not strongly dependent on the exact set of dynamical constraints: in the next subsections we show how it can be adapted to all KA models on hypercubic lattices.

2.1.4. Exponential Convergence of Frameability of Large Systems

We now show that the probability a configuration of a hypercube is frameable approaches one (at least) *exponentially fast* in its linear size L, i.e.

$$\mu_{\Lambda, \rho}(\mathcal{F}) \geqslant 1 - C \exp\left(-\frac{L}{\Xi^u}\right) \tag{11}$$

for $L \geqslant \Xi^u(\rho)$.

In addition to its direct relevance for the square lattice model, this result will be needed for analyzing other KA models. It is instructive to consider two ways of proving the exponential convergence.

   (i)   The first is via a percolation-like argument, in the same spirit as that used in ref. 43. Consider initially a square lattice Λ of linear size L, divide it into a set of smaller squares of linear sizes l and focus on one of them, Λ_ℓ. If the four neighboring squares of Λ_l are framed, then the $3l \times 3l$ square that includes all these small squares can also be framed (see Fig. 5); other combinations of the nine subsquares also suffice to make the larger square frameable.

   In this way one can grow large frameable squares. The crucial observation is that if the (possibly) unframeable subsquares do not span across the larger square, then the latter can definitely be framed. This condition is simply the *lack* of percolation of unframeable squares. Thus

$$1 - \mu_{\Lambda_L, \rho}(\mathcal{F}) \leqslant P_{\text{perc}}(L/l, \mu_{\Lambda_l, \rho}(\mathcal{F}), 2), \tag{12}$$

where $P_{\text{perc}}(l, r, 2)$ the probability of conventional site percolation for a square lattice of linear size l, with occupation probability $1 - r$. From site-percolation estimates[43]

$$P_{\text{perc}}(l, r, d) \leqslant \sum_{j=l}^{\infty} 4(1-r)^j 4^{j-1} = \frac{4}{3} \frac{(3(1-r))^{l-1}}{1 - 3(1-r)}. \tag{13}$$

Therefore, if for the sub-squares

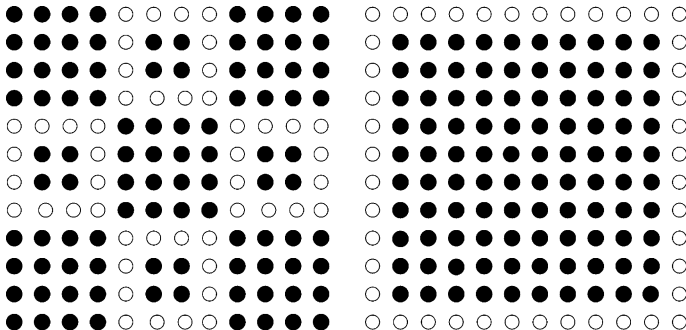$$\mu_{\Lambda_l, \rho}(\mathcal{F}) > 1 - \frac{1}{3e} \tag{14}$$

Fig. 5.   Construction of a large framed square from a partial set of framed subsquares: the two configurations can be connected by a sequence of moves similar to those of Fig. 2: starting from the corners that connect two empty edges one can move lines of vacancies up, down, right and left to reach the final configuration.

Eq. (12) and (13) imply that for the large square

$$\mu_{\Lambda,\rho}(\mathcal{F}) \geqslant 1 - Ce^{-L/l} \tag{15}$$

with a positive constant C. Since (14) holds for $l = \Xi$ – by the definition of the crossover length – the desired exponential bound, (11), is proven.

(ii) The second method is via a renormalization group (RG) approach (see ref. 44 for a similar argument in the context of bootstrap percolation). Consider a square lattice Λ_L of linear size L and divide it into four squares of linear size $L/2$. If at least three of the four subsquares are frameable, then the large square is also frameable. This implies an iterative inequality:

$$\mu_{\Lambda_{2L},\rho}(\mathcal{F}) \geqslant \left(\mu_{\Lambda_L,\rho}(\mathcal{F})\right)^4 + 4\left(\mu_{\Lambda_L,\rho}(\mathcal{F})\right)^3 (1 - \mu_{\Lambda_L,\rho}(\mathcal{F})) \tag{16}$$

If

$$1 - \mu_{\Lambda_L,\rho}(\mathcal{F}) \leqslant \frac{1}{10e} \tag{17}$$

then on the next scale up

$$\mu_{\Lambda_{2L},\rho}(\mathcal{F}) \geqslant 1 - 10(1 - \mu_{\Lambda_L,\rho}(\mathcal{F}))^2 \tag{18}$$

which implies that condition (17) holds also for $2L$. We can thus iterate the inequality (18) to obtain

$$\mu_{\Lambda_{2^n L},\rho}(\mathcal{F}) \geqslant 1 - 1/10 \left(10(1 - \mu_{\Lambda_L,\rho}(\mathcal{F}))\right)^{2^n} \geqslant 1 - \frac{1}{10}e^{-2^n} \tag{19}$$

Since for $L > \Xi(\rho)$ condition (17) holds, Eq. (19) gives the desired bound (15) for large square lattices.[8]

2.2. Irreducibility for $d = 3$, $s = 2$

We now turn to the double-vacancy-assisted cubic lattice case, $d = 3$, $s = 2$, that was originally studied by KA, and prove that configurations are almost surely in the same large irreducible component in the infinite system limit for any density. This case can be analyzed by the general discussion of Section (2.4) however the study of this more highly constrained

---

[8]Note that we have only considered $L = 2^n \Xi_{2,1}(\rho)$ for integer n, but the results can be readily extended to all L.

three-dimensional case is useful as it introduces, in a readily visualized situation, the technique we use to extend ergodicity results from smaller to larger values of d and s.

Consider a cubic lattice $\Lambda \in \mathbb{Z}^3$ with size L^3. Define *framed* configurations as those with all the boundary sites empty and define *frameable* as those that, by an allowed sequence of elementary moves, can reach a *framed* configuration. Again, frameable configurations with the same number of particles belong to the same irreducible component. This can be checked by noticing that the bottom and top planes of vacancies can be raised and lowered performing the same "sandwich procedure" as for the $d = 2$, $s = 1$ case, but here using empty planes instead of empty rows.

A lower bound on the probability that a configuration is frameable, $\mu_{\Lambda, \rho}(\mathcal{F})$, can be obtained by the following expansion argument. Consider a cube of linear size four, which has at its center an empty cube of linear size two. If adjacent to each face of the internal cube there is a 4×4 square that is frameable in the $d = 2$, $s = 1$, – single-vacancy-assisted planar — sense, the whole cube of size four is frameable in the desired three-dimensional double-vacancy-assisted sense. This procedure can be iterated to grow an $L \times L \times L$ frameable configuration from an empty cube of size two, by requiring that in each subsequent shell all six of the *square faces are frameable*.[9]

Letting $\mu_{\Lambda, \rho}(\mathcal{F}^0)$ be the probability of frameable configurations grown from a nucleus at the origin, a series of lower bounds for $\mu_{\Lambda, \rho}(\mathcal{F})$ follows beginning from a completely empty X^3 nucleus for general X

$$\mu_{\Lambda, \rho}(\mathcal{F}) \geqslant \mu_{\Lambda, \rho}(\mathcal{F}^0) \geqslant (1 - \rho)^{X^3} \prod_{l=X/2}^{L/2-1} \left(\mu_{\Lambda_{2l}, \rho}^{2,1}(\mathcal{F}) \right)^6 \quad \forall X \tag{20}$$

with Λ_{2L} is a $2L \times 2L$ square corresponding to one of the expansion faces. From the previous subsection we know that the frameable probability of a square, $\mu_{\Lambda, \rho}^{2,1}(\mathcal{F})$, is exponentially close to unity for $L \gg \Xi_{2,1}(\rho)$. As in the case of bootstrap percolation[(45)] choosing $X >> \Xi_{2,1}(\rho)$ in (20) makes the pre-factor dominate over the product and we conclude that

$$\mu_{\infty, \rho}(\mathcal{F}^0) \sim (1 - \rho)^{\Xi_{2,1}(\rho)^3} \tag{21}$$

---

[9]Actually we should require a little more than that all the square faces be frameable: one needs two frameable square of size $L \times L$, two of size $L \times L + 2$ and two of size $L + 2 \times L + 2$. We skip these details whose effects are subdominant compared to those we compute.

for $L \gg \Xi_{2,1}(\rho)$; this yields

$$\xi_{3,2}(\rho) \sim \Xi_{2,1}(\rho) \tag{22}$$

as the characteristic length scale above which the frameability conditions are met with high probability.

By considering the $O\left(L^3/\xi^3\right)$ possible initial nuclei in a large L^3 cube, we can show, by analogy with the two-dimensional case, that $\lim_{L \to \infty} \mu_{\Lambda,\rho}(\mathcal{F}) = 1$ thereby establishing an upper bound for the crossover length $\Xi_{3,2}(\rho)$ above which the large irreducible component dominates:

$$\Xi_{3,2}^u(\rho) \equiv \xi_{3,2}(\rho)(1-\rho)^{-\Xi_{2,1}^u(\rho)^3/3}. \tag{23}$$

Up to subdominant corrections, this means

$$\log \Xi_{3,2}^u(\rho) \sim [\Xi_{2,1}^u(\rho)]^3. \tag{24}$$

2.3. Irreducibility for all d, $s = 1$

We now extend the results derived in the previous two subsections. First we consider $s = 1$ on general hypercubic lattices.

As above, define *framed* configurations to be those with all their one-dimensional hyperedges empty and define as *frameable* those reachable from framed configurations. In the three-dimensional cubic case, for example, the relevant edges are the 12 edges of a cube. As in the cases already discussed, all framed configurations – and therefore also the corresponding frameable ones – belong to the same irreducible component. This can be seen, for example, in the cubic case, by considering permuting the occupation variables of two neighboring sites $\{i, j\}$ which lie in a plane parallel to the "bottom" plane. By starting from the corners, the bottom frame can be raised till it frames the plane that contains the pair $\{i, j\}$. Then, after applying on this plane the same sandwich technique used for single-vacancy assisted motion on a square lattice, the desired permutation can be performed and the frame then reexpanded and returned to the bottom plane.

The growing technique that enables the construction of larger frameable configurations starting from an empty nucleus, can be generalized via the following observation. Given a frameable hypercube of linear size L, to expand it to size $L + 2$, 2^{d-1} vacancies are needed in the subsequent shell for each of the 2^d hyperfaces. Therefore, the probability that a configuration is frameable, $\mu_{\Lambda,\rho}^{(d)}(\mathcal{F})$, can be bounded from below by $\mu_{\Lambda,\rho}^{(d)}(\mathcal{F}^0)$,

with

$$\mu_{\Lambda,\rho}^{(d)}(\mathcal{F}^0) = (1-\rho)^{2d} \prod_{l=2}^{\infty} \left(1 - \sum_{j=0}^{2^{d-1}-1} \frac{l^{d-1}!}{(l^{d-1}-j)!j!} \rho^{l^{d-1}-j}(1-\rho)^j \right)^{2^d},$$

(25)

where the product is over even l. In the limit $\rho \to 1$, $L \to \infty$

$$\mu_{\Lambda,\rho}^{(d)}(\mathcal{F}^0) \sim \exp\left(-\frac{c(d)}{(1-\rho)^{\frac{1}{d-1}}} \right),$$

(26)

where

$$c(d) = -2^{d-1}(d-1) \int_0^1 \frac{dy}{y(\log y)^{\frac{d-2}{d-1}}} \log\left(1 - y \left(\sum_{j=0}^{2^{d-1}-1} \frac{(-\log y)^j}{j!} \right) \right).$$

(27)

As for the square case, there exists a length

$$\xi(\rho, d, 1) \approx (-\log(1-\rho)/(1-\rho))^{1/(d-1)}$$

(28)

such that $\mu_{\Lambda,\rho}^{(d)}(\mathcal{F}^0)$ varies little with L for $L \gg \xi$. Therefore, by considering the $O\left(L^d/\xi^d\right)$ possible distinct positions for the nucleus, an upper bound for the cross-over length follows

$$\Xi_{d,1}^u(\rho) \sim \exp\left(\frac{c(d)}{d(1-\rho)^{\frac{1}{d-1}}} \right).$$

(29)

As explained at the end of Section 2.1, requiring that the number of possible positions for framing nuclei times the probability that the configuration is frameable about a given nucleus is of order one, is not enough to conclude that $\mu_{\Lambda,\rho}(\mathcal{F}) = 1$. Again, the conditions that a configuration is frameable about two different nuclei, are not independent events. However, provided the nuclei are sufficiently far apart, these events are almost independent since the frameability requirements become weaker and weaker for larger sizes. Indeed the requirement to have at least $2^d - 1$ vacancies on each of the 2^d faces of a frameable hypercube only amounts to $2^d - 1$ vacancies among L^{d-1} sites and thus, at fixed density, this becomes less and less restrictive at larger sizes.

We outline an iterative argument by which the desired previous result can be proved (see Ref. 44 for a similar argument for bootstrap percolation). Divide the lattice into $(L/l_2)^d$ hypercubes of linear size l_2. At the center of each of these hypercubes consider a smaller hypercube Λ_1 of size $l_1 = l_2/2$. The probability that the lattice is frameable can be bounded using the probability that the lattice can be made frameable starting from one of the $(L/l_2)^d$ hypercubes of linear size l_1. We thus have a bound $\mu_{\Lambda,\rho}(\mathcal{F}) \geqslant P_1 P_2 P_3$, in terms of the probabilities of three events: P_1, the probability that at least one of the hypercubes of size l_1 is frameable; P_2, the probability that this frameable hypercube can be expanded until the size l_2 (requiring 2^{d-1} vacancies for each shell from size l_1 to size l_2); and P_3, the probability that the frameable hypercube of size l_2 can be expanded until the size L requiring 2^{d-1} vacancies on each shell from size l_2 to L *excluding* the regions of space occupied by the other small hypercubes of size l_1. The following results can be readily derived:

$$P_1 = 1 - (1 - \mu_{\Lambda_1,\rho}(\mathcal{F}^0))^{\frac{L^d}{l_2^d}} \simeq 1 - \exp\left(-\mu_{\Lambda_1,\rho}(\mathcal{F}^0)\frac{L^d}{l_2^d}\right),$$

$$P_2 = \prod_{l=l_1}^{l_2}\left(1 - \sum_{i=0}^{2^{d-1}-1}\binom{l^{d-1}}{i}\rho^{l^{d-1}-i}(1-\rho)^i\right)^{2^d},$$

$$P_3 = \prod_{l=l_2}^{L}\left(1 - \sum_{i=0}^{2^{d-1}-1}\binom{(l/2)^{d-1}}{i}\rho^{(l/2)^{d-1}-i}(1-\rho)^i\right)^{2^d}. \tag{30}$$

By choosing $l_1 \approx \xi(\rho, 1, d)$, these give

$$P_1 \approx 1 - \exp\left(-\exp\left(-\frac{c(d)}{(1-\rho)^{\frac{1}{d-1}}}\right)\frac{L^d}{l_2^d}\right),$$

$$P_2 \approx 1,$$

$$P_3 \approx 1 \tag{31}$$

so that $\mu_{\Lambda,\rho}(\mathcal{F})$ is of order unity as long as $\exp(-c(d)/(1-\rho)^{1/(d-1)})$ $(L/l_2)^d \gg 1$, i.e. for $L \gg \Xi_{d,1}^u(\rho)$ with $\Xi_{d,1}^u(\rho)$ given by Eq. (29).

2.4. Irreducibility for all *d* with *s* < *d*

We now consider KA models with general parameter $0 < s < d$ on a hypercubic lattices of dimension d. These are the non-trivial cases. (As

mentioned earlier, or $s \geqslant d$, any completely occupied d-dimensional hyper-cubes are frozen so that these KA models on hypercubic lattices are non-ergodic for any density $\rho > 0$. At the opposite extreme, $s = 0$ is the normal lattice gas which is trivially ergodic.)

The $s = 1$ case was considered in the previous subsection. We now show how the general case can be analyzed, and irreducibility proved, via a generalization of the iterative procedure used in Section 2.2 to extend the $d = 2$, $s = 1$ results to $d = 3$, $s = 2$.

Define *framed* configurations of d-dimensional hypercubes as those with all hyperedges of dimension s empty. (More formally the configurations with no particles on the hyperplanes:

$$\{x_{E_1} = 1, L\} \times \{x_{E_2} = 1, L\} \times \cdots \{x_{E_{d-s}} = 1, L\} \qquad (32)$$

where $E_1, \ldots E_{d-s}$ for all sets of $d - s$ of the indices $1, \ldots, d$.) Inside a frameable hypercube, any move of a particle to a neighboring empty site can be achieved by the generalization of the sandwich technique discussed previously.

Consider a frameable hypercube of size l. If adjacent to each hyper-face there is a $d - 1$-dimensional hypercube that is frameable in the $d - 1$, $s - 1$ sense, then the enclosing d-dimensional hypercube of size $l + 2$ is frameable. Therefore, to bound from below the frameable probability, $\mu_{\Lambda, \rho}(\mathcal{F}^{(d,s)})$, we need to estimate the probability that a hypercube of linear size X centered at the origin is empty and that expanding from it any subsequent shell is frameable in the $d - 1$, $s - 1$ sense. This yields

$$\mu_{\Lambda^d, \rho}(\mathcal{F}^0_{(d,s)}) \geqslant (1 - \rho)^{X^d} \prod_{\ell = X+1}^{L} \mu_{\Lambda_\ell, \rho}(\mathcal{F}_{(d-1,s-1)}), \qquad (33)$$

where Λ_ℓ^{d-1} is a $d - 1$-dimensional lattice of linear size ℓ. The argument given is Section 2.1.4 for $d = 2, s = 1$ can be extended to the get that the convergence of the frameable probability to one is exponential in the linear size of the system and determined by $\Xi^u_{d-1, s-1}(\rho)$[10]

$$\mu_{\Lambda, \rho}(\mathcal{F}_{(d-1, s-1)}) \geqslant 1 - C \exp\left[L / \Xi^u_{d-1, s-1}\right] \quad \text{for} \quad L \gg \Xi^u_{s-1, d-1}(\rho). \tag{34}$$

[10]Note that the argument for exponential convergence requires the *a priori* knowledge of convergence to unity for the probability of the frameble component. This has been proven for any d, $s = 1$ in previous section. Therefore (34) holds for any d, $s = 2$ and the argument below leads to $\mu_{\infty, \rho} = 1$ for these cases. Therefore, one can apply again arguments in Section 2.1.4 and obtain exponential convergence for all the cases $s = 2$, i.e. (34) for $s = 3$. And so on iteratively.

Hence, by choosing $X \gg \Xi_{s-1,d-1}^u(\rho)$, the product on ℓ in (33) is close to unity. From generalization of the arguments given for the $s=1$ square lattice case, a non-zero probability of frameability around a given nucleus that converges rapidly to its asymptotic limit for large sizes implies a probability close to unity for frameability of sufficiently large hypercubes around *some* nucleus. More precisely that $\mu_{\Lambda,\rho}(\mathcal{F}_{(d,s)})$ approaches unity in the thermodynamic limit and is close to one for $L \gg \Xi_{d,s}^u(\rho)$. Since the dominant small factor in (33) is the large power of $1-\rho$, and to make frameability likely one needs a system large enough to contain at least one frameable hypercube of size greater than $\Xi_{d-1,s-1}^u$, an upper bound on the crossover length is

$$\Xi_{d,s}^u(\rho) \sim \left[(1-\rho)^{-\Xi^u(\rho,d-1,s-1)^d} \right]^{\frac{1}{d}}. \tag{35}$$

From the earlier results for $s=1$ in general $d \geqslant 2$, we know $\Xi_{d1}^u(\rho)$: Eq. (29). Therefore, by induction, Eq. (35) yield upper bounds for the crossover length for general s, d with $1 < s < d-1$. The density dependence of this upper bound, Ξ^u, is hence

$$\Xi^u(\rho, s, d) = \exp^{\circ s} \frac{C(d,s)}{(1-\rho)^{1/(d-s)}}, \tag{36}$$

where $\exp^{\circ s}$ denotes the exponential function iterated s times. Note that the factors of $\ln(1-\rho)$ that appear in 35 can be taken into account, as far as the upper bound, by a slight modification of $C(d,s)$.

2.5. Ergodicity for all *d* with *s* < *d*

Thus far, we have only considered the irreducibility of configurations in infinite systems. In this section we prove that the almost-sure existence of an irreducible component in the thermodynamic limit implies ergodicity (i.e., the third step of the procedure outlined in Section 2.1). We follow the same strategy as in section 4 of ref. 46. Since the proof is the same for any of the models, we temporarily drop the indices d and s. It is first necessary to introduce some mathematical notation and give a rigorous definition of ergodicity for infinite systems.

Define $\Omega_\Lambda \equiv \{0,1\}^{|\Lambda|}$ as the configuration space of the hypercubic lattice $\Lambda \in \mathbb{Z}^d$ and configurations η as the elements of Ω, namely sets of occupation numbers $\eta_x \in \{0,1\}$ for $x \in \Lambda$. The dynamics of KA models is a continuous time Markov process with generator $\mathcal{L}$ acting on local functions $f : \Omega_\Lambda \to \mathbb{R}$ as

$$\mathcal{L}f(\eta) = \sum_{\substack{\{x,y\} \subset \Lambda \\ |x,y|=1}} \eta_x(1-\eta_y)c_{xy}(\eta)\left[f(\eta^{xy}) - f(\eta)\right] \tag{37}$$

with the sum running over nearest neighbor pairs, x, y. The quantity in square brackets,

$$\nabla_{xy}f \equiv f(\eta^{xy}) - f(\eta), \tag{38}$$

acts to change the occupation of sites x and y so that the occupation number of the zth site in configuration η^{xy} is related to the occupations in the configuration η by

$$\eta_z^{x,y} := \begin{cases} \eta_y & \text{if } z=x \\ \eta_x & \text{if } z=y \\ \eta_z & \text{if } z \neq x, y \; ; \end{cases} \tag{39}$$

The jump rates $c_{x,y}(\eta)$ encode the constraints imposed by the KA rules, namely

$$c_{xy}(\eta) := \begin{cases} 1 & \text{if } n_x^{\bar{y}}(\eta) \leqslant m \text{ and } n_y^{\bar{x}}(\eta) \leqslant m, \\ 0 & \text{otherwise} \end{cases} \tag{40}$$

where

$$n_x^{\bar{y}}(\eta) := \sum_{\substack{z \in \Lambda, \; z \neq y \\ |x-z|=1}} \eta_z, \tag{41}$$

i.e. $n_x^{\bar{y}}(\eta)$ is the number of occupied neighbors of x, excluding y.

The dynamics preserves the number of particles, (i.e. the subspaces with fixed number, N, of particles $\Omega_{\Lambda,N} := \{\eta \in \Omega_\Lambda \sum_{x \in \Lambda} \eta_x = N\}$ are invariant and the uniform measure $\nu_{\Lambda,N}$ on fixed N subspaces is invariant). However, due to the vanishing of certain rates for $m < 2d - 1$ ($s \geqslant 1$), the configuration space, $\Omega_{\Lambda,N}$, of finite lattices breaks into disconnected components: the Markov chain is hence reducible so that the process is not ergodic on these subspaces. On the other hand, for the infinite lattice $\Lambda = \mathbb{Z}^d$, the process satisfies detailed balance with respect to the trivial Bernoulli product measure, μ_ρ, at any density ρ. Moreover, from the previous section, we know that there exists an irreducible component – the set of frameable configurations – that covers the configuration space. However this is not

enough to conclude that the system is ergodic. Indeed, while for finite state systems irreducibility of the Markov chain implies that there exists a unique invariant measure and the system is ergodic with respect to it, this is not *a priori* true in infinite systems. For example, Ising models below their critical temperature are irreducible but not ergodic in zero field because of the coexistence of the two phases each of which lasts for infinite time. To establish ergodicity for infinite systems, one needs to prove[30] that the long-time limit of all correlation functions – weighted averages over the probability distribution at time t, $\mathcal{P}_t = \mathcal{P}_t \sim \exp \mathcal{L}t$ – approaches those of the Bernoulli product measure for almost all initial conditions, η^I: more precisely that

$$\lim_{t \to \infty} \int d\mu_\rho(\eta^I) \big[\mathcal{P}_t f(\eta^I) - \mu_\rho(f)\big]^2 = 0 \quad \forall f \in L_2(\mu_\rho) \ ,$$

where $f \in L_2(\mu_\rho)$ if $\int d\mu_\rho(\eta) f^2(\eta) < \infty$ and $\mu_\rho(f)$ is the equilibrium average of function f, namely

$$\mu_\rho(f) \equiv \int d\mu_\rho(\eta) f(\eta) \ , \tag{42}$$

and $\mathcal{P}_t f(\eta^I)$ is the correlation function $f(\eta)$ averaged over all possible histories up to time t starting with initial configuration η^I.

By the spectral theorem, convergence to the equilibrium measure occurs if and only if zero is a *simple* eigenvalue of the generator of the dynamics, $\mathcal{L}$, i.e. if the only functions, f_0, in $L_2(\mu_\rho)$ for which $\mathcal{L}f_0(\eta) = 0$ are constant on almost all configurations, i.e. on all except possibly a set of measure zero.[30] Note that if the system can be trapped for an infinite time in some region of the configuration space, this would not be true: the characteristic function of this region would be a non-constant eigenvector of $\mathcal{L}$ with zero eigenvalue. This corresponds to the natural idea that ergodicity breaking is related to the existence of regions of the configuration space that are effectively disconnected. In the Ising model case, the function $f(\eta)$ that is equal to unity on configuration η if a majority of the sites have up spins, and equal to zero otherwise, is such an example. The strategy of the proof of ergodicity of KA models on infinite hypercubic lattices $\mathbb{Z}^d$ with parameter s such that $s < d$ is the following. (1) First we prove that, if f_0 is eigenvector of $\mathcal{L}$ with zero eigenvalue, $f_0(\eta) = f_0(\eta^{x,y})$ almost surely with respect to μ_ρ for any pair of sites $\{x, y\}$, i.e. $\mu_\rho([f_0^{xy} - f_0]^2) = 0$ where $f_0^{xy}(\eta) \equiv f_0(\eta^{x,y})$. This part of the proof uses as a key ingredient the existence of an irreducible component which has unit probability in the thermodynamic limit. (2) Then we use the fact that symmetric measures can be decomposed on product measures (De Finetti's theorem[47,48]) to conclude that any such f_0 is in fact constant.

Let us prove (1). By enumerating frameable configurations, η^1, η^2, ... η^n, ..., we can rewrite the event that a configuration is frameable as $\mathcal{F} := \bigcup_{n \geqslant 1} \eta^n$ and define the function $\mathbb{1}_{\mathcal{F}}$ to be one if $\eta \in \mathcal{F}$ and zero otherwise. The result $\mu_\rho(\mathcal{F}) = 1$ established in previous sections implies

$$\mu_\rho([\nabla_{xy}f]^2) = \mu_\rho([\nabla_{xy}f]^2 \mathbb{1}_{\mathcal{F}}) \leqslant \sum_{n=1} \mu_\rho([\nabla_{xy}f]^2 \mathbb{1}_{\eta^n}) \quad \forall f \in L_2(\mu_\rho), \quad (43)$$

where the exchange operator ∇_{xy} was defined in (38). From the properties of frameable configurations, for any configuration $\eta \in \mathcal{F}$ one can always find a path η, η^1, ..., η^M with $\eta^M = \mu^{xy}$ that connects η to η^{xy} through allowed moves, i.e. with $\eta^{i+1} = \eta^{i;zw}$ for some pair of neighboring sites $\{z, w\}$ and $c_{zw}(\eta^i) = 1$. By telescoping sums and the Cauchy–Schwartz inequality,[11] each term in the sum (43) can now be bounded from above by a sum of elementary exchanges allowed by KA rules, i.e. terms $\mu_\rho(c_{zw}[\nabla_{zw}f]^2)$. Note that we can introduce the jump rate in the upper bound only since, as written above, we can choose elementary moves with rate equal to one (never to zero). This is thanks to the fact that the frameable component has unit probability, thus we could restrict the mean in (43) as a mean over the frameable component, where we know that a path of allowed moves exists for sure. The hypothesis of sentence (1), namely that there is some f_0 that is an eigenvector of $\mathcal{L}$ with zero eigenvalue, implies that $\mu_\rho(f_0 \mathcal{L} f_0)$ is zero. Moreover, the symmetry $c_{xy}(\eta) = c_{yx}(\eta)$ – the microscopic reversibility – implies

$$\mu_\rho(f_0 \mathcal{L} f_0) = -\frac{1}{2} \sum_{\{x,y\} \in \mathbb{Z}^d} \mu_\rho \left(c_{xy}(\eta) [\nabla_{xy} f_0]^2 \right). \quad (44)$$

Since the right hand side of (43) can be rewritten as a sum of such terms, the fact that $\mu_\rho(f_0 \mathcal{L} f_0) = 0$ implies $\mu_\rho([\nabla_{x,y} f_0]^2) = 0$ and completes the proof of (1).

We now turn to the proof of (2). Consider the measure $\tilde{\mu}^{f_0}$ defined as $\tilde{\mu}^{f_0}(\eta) \equiv f_0^2(\eta) \mu_\rho(\eta) / \mu_\rho(f_0^2)$. Since μ_ρ is symmetric under exchanges

---

[11] Note that for any frameable configuration the existence of a path that joins η and $\eta^{x,y}$ is guaranteed. However, its length can be arbitrarily large on some rare configurations. Therefore, strictly speaking, one cannot directly apply Cauchy–Schwartz inequality which would pull out a non-bounded factor proportional to the length of the maximal path. However, by dividing frameable configuration on sets characterized by the length ℓ of the minimal path (to perform such move), it is possible to bound each term in the r.h.s. of (43) as an infinite sum (on ℓ) of terms of the kind ℓ multiplied by terms $\mu_\rho(c_{zw}[\nabla_{zw}f]^2)$. This, together with the observation (see below) that each of this terms must be equal to zero, is sufficient to conclude that the l.h.s. in (43) is equal to zero.

of particles and vacancies, i.e. $\mu_\rho(\eta) = \mu_\rho(\eta^{x,y})$, and $f_0(\eta^{xy}) = f_0(\eta)$ on almost all the configuration space, $\tilde{\mu}^{f_0}$ is also symmetric, i.e. $\tilde{\mu}^{f_0}(\eta) = \tilde{\mu}^{f_0}(\eta^{x,y})$ for any η and any pair $\{x, y\}$. Thanks to De Finetti theorem[47,48] a symmetric measure can be always decomposed on product measures corresponding to different densities. However, measures corresponding to different densities are concentrated on different sets of configurations. Hence, all the coefficients of the decomposition of $\tilde{\mu}^{f_0}$ on product measures have to be zero except the one corresponding to μ_ρ. Therefore $f_0^2(\eta)/\mu_\rho(f_0^2) = 1$, which implies that $f_0(\eta)$ is constant[12] and equal to the coefficient of the decomposition corresponding to μ_ρ.[13]

3. QUANTITATIVE RESULTS

In previous sections we have proven that for any parameters d and s, with $s < d$, ergodicity holds in the thermodynamic limit. Moreover, we have determined an upper bound $\Xi_{d,s}^u(\rho)$ for the density dependent cross over length, $\Xi_{d,s}(\rho)$, that separates two different regimes on finite volume hypercubes $\Lambda \in \mathbb{Z}^d$ of linear size L: if $L \to \infty$ and $\rho \to 1$ with $L \geqslant \Xi_{s,d}(\rho)$, than $\mu_{\Lambda,\rho}(\mathcal{M}) \to 1$; if $L \to \infty$ and $\rho \to 1$ with $L \geqslant \Xi_{s,d}(\rho)$, than $\mu_{\Lambda,\rho}(\mathcal{M}) \to 0$, where $\mathcal{M}$ is the maximal irreducible component (i.e. set of configurations on Λ connectable by possible path which has larger probability w.r.t. Bernoulli measure at density ρ, $\mu_{\Lambda,\rho}$). In other words, for $L \ll \Xi_{s,d}(\rho)$ the configuration space is dominated by a single ergodic component, while for $L \ll \Xi_{s,d}(\rho)$ different components contribute.

In the next subsection we find a *lower bound* $\Xi_{d,s}^l(\rho)$, which has the same form of density dependence as the upper bound. In the Sections 3.2, 3.3 we show that for specific cases, the exact asymptotic behavior of the crossover length can be obtained – including the numerical coefficients.

3.1. Bootstrap Percolation and Lower Bounds on Crossover Length

In this subsection we explain how one can obtain a lower bound on the crossover length, Ξ, thanks to a relation among KA models and the well studied problem of *bootstrap percolation*.

---

[12]Since this procedure can be repeated for any linear combination of $f_0(\eta)$ with the constant function, we obtain that the square of any linear combination of $f_0(\eta)$ with the constant function is a constant which implies that $f_0(\eta)$ is indeed itself constant.

[13]Note that for Ising models at low temperature in zero field we cannot invoke such a unique decomposition (the hypothesis for De Finetti's theorem do not hold since the equilibrium measure is not simply a product) and therefore $\mu_\rho([f_0^{x,y} - f_0]^2)$ does not imply that f_0 is constant.

Consider a random configuration at density ρ on a d-dimensional hypercubic lattice Λ. One can isolate frozen subsets (possibly empty) of such a configuration by the following deterministic procedure. First remove all the particles that have no more than m neighbors, then iterate this procedure until no more particles can be removed. Indeed, as already noticed by KA for the $d=3$ $s=2$ case, all the particles (if any) that remain at the end of such procedure are frozen: namely they can never move under KA dynamics starting from the original configuration.[14] This procedure is simply related to conventional bootstrap percolation (refs. 49–50) which corresponds to starting from a configuration at density ρ, iteratively *adding* particles in empty sites that have fewer than m neighbors, and considering any clusters of empty sites that may remain at the end of this process. In other words, by exchanging particles and vacancies, and hence ρ with $1 - \rho$, one recovers the usual bootstrap procedure. Let $\mu^B_{\Lambda,\rho}$ be the probability that, starting from a random configuration on an hypercube $\Lambda \in \mathbb{Z}^d$ of linear size L, a cluster of particles remains at the end of the modified bootstrap procedure we are interested in. The rigorous results in ref. 43 for usual bootstrap percolation yield the existence of a crossover length $\Xi^B(\rho, d, s) \equiv \exp^{\circ s}(K(d,s)/(1-\rho)^{d-s})$ such that if one sends simultaneously $\rho \to 1$ and $L \to \infty$ with L growing faster (slower) than Ξ^B, $\mu^B_{\Lambda,\rho}$ goes to one (zero). Furthermore, the convergence to unity in the regime for $L > \Xi^B(\rho, d, s)$ is exponentially fast.

To our knowledge only upper and lower bounds on the constant $K(d,s)$ are available in the general case, while the exact value has been recently determined[52] for the case corresponding to our $d=2$, $s=1$. For the non-trivial models, $s < d$, if clusters of particles remain, they must be system-spanning clusters (i.e. clusters that connect two boundaries of the system): in infinite systems, such frozen clusters must be infinite. Since on any finite lattice two configurations with different frozen sets belong to different irreducible components, the likely presence of such system-spanning clusters of frozen particles we have immediately that when $\rho \to 1$ and $L \to \infty$ with L increasing slower than $\Xi^B(\rho, d, s)$, the probability of the maximal irreducible component for KA model $(\mu_{\Lambda,\rho}(\mathcal{M})$ is strictly smaller than one. This corresponds to the following lower bound for the KA crossover length:

$$\Xi_{d,s}(\rho) \geqslant \Xi^l_{d,s}(\rho) = \Xi^B(\rho, d, s) \ . \tag{45}$$

---

[14]Note that the converse is not guaranteed: *a priori* there could exist sets of particles that are thrown away during the deterministic procedure, but they are forever blocked under KA dynamics.

Note that the form of the density dependence of this lower bound (45) is the *same* as that of the upper bound, (36).

As mentioned above, for the case $d=2$, $s=1$, recent results have been found in ref. 52 with a sharp value of the constant: $K(2, 1) = \pi^2/18$. On the other hand, from Eq. (10) we find $C(2, 1) = - \int_0^1 dy \frac{\log(1 - y + y \log y)}{y} \simeq 4.4$, therefore $K(2, 1) < C(2, 1)$ and $\Xi_{2,1}^u(\rho) > \Xi_{2,1}^l(\rho)$. In the next subsection we show how, from a different framing technique, it is possible to determine a stronger upper bound for $\Xi_{2,1}(\rho)$ which turns out to be equal to the lower bound from bootstrap percolation.

3.2. Optimal Framing and Exact Crossover Length for $d=2$, $s=1$

We now show how exact results for the crossover length of the single-vacancy assisted ($s=1$) KA model on a square lattice can be obtained by an optimal framing construction.

Define a $W \times H$ rectangle (with $W + H$ even) to be *optimally framed* if it has $\frac{1}{2}(W + H) + 1$ vacancies arranged with one in a corner and the others on alternate sites of the two perpendicular sides that intersect at that corner, plus any number of additional vacancies, see Fig. 6. *Optimally frameable* configurations are those that can be reached from an optimally framed configuration with allowed moves.

One can show that all optimally framed configurations of a rectangle with the same particle number belong to the same irreducible component. Hence all the optimally frameable configurations belong to the same irreducible component. This follows by showing that within an optimally frameable rectangle any nearest neighbor pair of particles can be exchanged and all the other particles returned to their starting positions. The sequence of moves to perform a generic such exchange can be constructed by considering the basic moves in Fig. 7, which allow one to
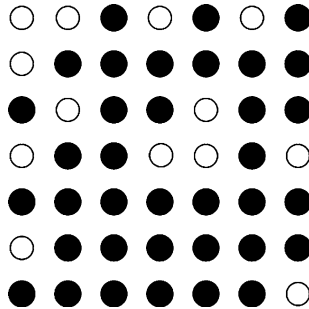

Fig. 6.   A 7×7 optimally framed configuration.
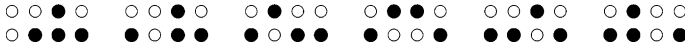
Fig. 7. Basic moves by which the three vacancy corner can move along the alternating-vacancy row of an optimally frameable rectangle.
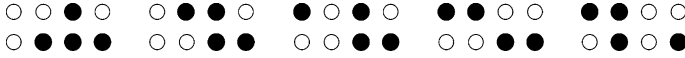

Fig. 8. Basic moves by which the row of alternating vacancies in an optimally frameable rectangle can be lowered.

move the nucleus of three vacancies along the row containing alternating vacancies, and those in Fig. 8 which enable one to lower and raise the row of alternating vacancies through the lattice. It is straightforward to check that with fewer than $1 + \frac{1}{2}(W + H)$ vacancies, large scale rearrangements of the particles in a rectangle are not possible: this suggests that this framing is, at least in some senses, optimal.

Following the same strategy as for the simple framing used previously, we now show how larger optimally frameable rectangles can be constructed. Consider an optimally framed $W \times H$ rectangular region embedded in a larger system. The following statements can be checked by direct inspection: if there is a vacancy in a line next-nearest neighbor to one of the rectangular edges parallel to either of the directions x or y, the rectangle can be expanded to a $W \times (H + 2)$ or $(W + 2) \times H$, respectively, optimally framed rectangle; if there is a vacancy in the line segment next to one of the rectangle's edges it is likewise *expandable* into a $W \times (H + 1)$ or $(W + 1) \times H$ framed rectangle; and if there is a vacancy next nearest neighbor along a *diagonal* from one of its corners, the rectangle is expandable to a $(W + 1) \times (H + 1)$ optimally framed rectangle.

Starting from a nucleus of three vacancies in a two-by-two square, the described expansion procedure can be iterated to grow larger frameable rectangles as long as the needed vacancies are present at each step. We must now estimate the probability that all the needed vacancies to construct an infinite frameable region centered on a chosen site are present. Define Q_k^ℓ as the probability that, given a $k - 2 \times l$ optimally frameable rectangle, it can be expanded to the right to an optimally frameable $k \times l$ rectangle which now includes the $(k - 1)$th and kth columns. From the above observations, we obtain the following recursion relations

$$Q_{k+2}^\ell = Q_{k+1}^\ell (1 - e^{-v\ell}) + Q_k^\ell e^{-v\ell}(1 - e^{-v\ell}) \tag{46}$$

where we have approximated, in the high density limit of interest, $\rho^\ell \simeq e^{-\ell(1-\rho)}$ (and used the notation $v = 1 - \rho$). Defining the ratios of successive

Qs by

$$R_k^\ell \equiv \frac{Q_{k+1}^\ell}{Q_k^\ell} \tag{47}$$

we obtain

$$R_{k+1}^\ell = (1 - e^{-v\ell}) + \frac{e^{-v\ell}(1 - e^{-v\ell})}{R_k^\ell} . \tag{48}$$

Since the least unlikely way for the rectangle to expand is roughly isotropically – as can be shown – we expect $k \approx l$ at large scales . Moreover, for k and l large the ratios of probabilities for successive expansions along the same axis will vary slowly, therefore a natural – and checkable – ansatz is

$$R_{k+1}^\ell \approx R_k^\ell \approx R(\ell). \tag{49}$$

By substituting (49) in (48), we find

$$R(\ell) \simeq \frac{1 - \mathcal{E}}{2} + \frac{1}{2}\sqrt{1 + 2\mathcal{E} - 3\mathcal{E}^2}. \tag{50}$$

where

$$\mathcal{E} = e^{-v\ell}. \tag{51}$$

As the rectangle has to be expanded to infinity in all four directions concurrently, this yields an estimate for the probability $\mu_{\infty,\rho}(\mathcal{O})$ that a specific nucleus of three vacancies can be expanded to an infinite optimally frameable rectangle

$$\mu_{\infty,\rho}(\mathcal{O}) \sim \left[\prod_{n=1}^{\infty} R(2n)\right]^4 \sim \exp\left[2\sum_{\ell=1}^{\infty} \ln R(\ell)\right] \tag{52}$$

which, by replacing the sum over ℓ by an integral and changing variables, yields

$$\mu_{\infty,\rho}(\mathcal{O}) \simeq \exp -\frac{2c_\infty}{1 - \rho} \tag{53}$$

with the constant given by

$$c_\infty = -\int_0^1 \frac{d\mathcal{E}}{\mathcal{E}} \ln\left[\frac{1 - \mathcal{E}}{2} + \frac{1}{2}\sqrt{1 + 2\mathcal{E} - 3\mathcal{E}^2}\right] = \frac{\pi^2}{18} \cong 0.55 . \tag{54}$$

The knowledge of $\mu_{\infty,\rho}(\mathcal{O})$ gives, as in previous sections, an upper bound for the crossover length

$$\Xi_{2,1}(\rho) \leqslant \exp \frac{c_\infty}{(1-\rho)}. \tag{55}$$

Since the constant c_∞ (54) has exactly the same value as the bootstrap constant $K(1,2)$ in ref. 52, the upper bound for Ξ obtained by the above framing procedure coincides with the lower bound provided by bootstrap results, thus giving the *exact* asymptotic high density behavior of the crossover length, up to subdominant pre-factors. This proves that the optimal framing procedure captures the dominant mechanism that restores ergodicity in large systems at high densities; this justifies referring to it as *optimal framing*.

3.3. Optimal Framing for $d=3$, $s=2$

We have shown that the framing procedure devised in Section 2.1 for the two-dimensional case is not optimal: indeed it does not capture the dominant ergodicity restoring mechanisms and therefore gives a non-optimal bound for the crossover length, Ξ. (see also Section 4). However, we were able to construct a different framing procedure which does capture the dominant mechanism. This was done through the construction of a lower-dimensional *basic structure* (lines of alternated particles and vacancies) in which each particle is blocked but only barely so: an *additional lower-dimensional vacancy cluster* (an extra vacancy in the square lattice case) can be moved throughout the whole structure.

We now construct a framing that we conjecture is optimal for the $d=3$, $s=2$ case. Consider a cube of linear size L which is completely filled with the exception of a plane $L \times L$ on which the configuration is given by the repetition of the unit cell of eight sites drawn in Fig. 9. It is possible to check that all the particles on such a plane can never move. However, if one adds two vacancies in place of e.g. the first particles on the two rows of one of the cells, then all the particles on the plane can be moved. Consider a cube which has three orthogonal faces with the above defined basic planar structure. We conjecture that with an extra set of $O(L)$ vacancies associated with the linking edges and $O(1)$ with the corner, the planar structures can be moved all across the cubic lattice and allow any exchange inside, i.e. they play the same role as the completely empty faces of frameable cubes defined in 2.2. If this is correct, by requiring $9/8L^2 + O(L)$ vacancies one can construct a configuration for a cube of linear size L in which all exchanges are allowed. We conjecture this to
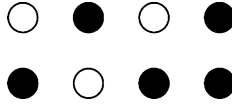
Fig. 9. Rectangular unit cell for the basic planar structure for the $d = 3$, $s = 2$ case.

be the minimal requirement, i.e. the above defined framing procedure to be the optimal one.

Note that the calculation of the probability for such a framing procedure to be expandable should yield an upper bound on the crossover length which is better than, although of the same form as, the one we obtained in (23), since fewer vacancies are required in successive layers. However, a rigorous lower bound – and hence the putative exact value of $C(3, 2)$ if the framing described here is indeed optimal – is not known; the exact value of $K(3, 2)$ for the corresponding bootstrap percolation has not been determined.[15]

4. PHYSICAL PICTURE OF THE COOPERATIVE KA DYNAMICS AT HIGH DENSITY

In this section, for completeness, we summarize the physical picture that we derived for the high density dynamics of the KA. This has already been discussed in ref. (40) and the derivation of some results on the dynamics will be presented in a forthcoming publication.[(53)] We focus for simplicity on the $s = 1$, $d = 2$ case leaving discussion of the natural generalization to any of the $s < d$, KA models on hypercubic lattices to the end.

As already noted, there are no finite clusters of vacancies that can freely move in an otherwise completely filled lattice. However, in a frameable region of size $l = \xi \sim \ln(1/(1-\rho))/(1-\rho)$, we know that: (1) all particle configurations inside the region can be reached from each other via an allowed (although long) path of elementary moves; (2) a frameable region can move of one step in a given direction if the surrounding configuration contains the minimal number of vacancies required to expand the region in the same direction in the framing procedure (see Section 3.2). Indeed, by using again the basic moves in Figs. 6 and 7, it is possible to construct a path that shifts the region of one step (the paths goes first

---

[15]Note that knowledge of $C(3, 2)$ from framing arguments would give a new upper bound on the value of $K(3, 2)$ for the Bootstrap problem and perhaps a hint of its exact value (recall that $K(2, 1)$ coincides with the constant coming from the correspondent KA problem calculated with the optimal framing).

through the expansion of the region, then the vacancies are left behind on the opposite side and the region moves); (3) a frameable region of size $\ell = \xi \sim \ln(1/(1-\rho))/(1-\rho)$ is likely to find at least one vacancy in each of ℓ consecutive line segments along each of the lattice directions. Thus frameable regions of size ξ can expand and, hence move, ξ steps, a distance similar to their diameter. For this reason, we refer to them as mobile cores,[40] although it may be a bit misleading, they have been called defects in other contexts.

The motion of frameable cores is, on long scales, like simple diffusion in a random medium. The size of mobile cores, $\ell = \xi \sim \ln(1/(1-\rho))/(1-\rho)$, is such that the random environment seen by the cores is the minimal one in which diffusion is possible. For smaller values of ℓ the probability to find the necessary vacancies in the neighborhood of a core is too low to guarantee that it can diffuse. In contrast larger frameable regions with $\ell > \xi$ could diffuse, but these would contribute less to the long-time dynamics because they are both rarer and move more slowly than cores of size ξ. (Indeed, larger frameable regions will tend to decompose into one (or more) minimal mobile cores, and leftover vacancies that cannot move without assistance of a mobile core.)

The diffusion coefficient of a tagged particle, D_S, one of the key physical quantities analyzed in simulations and experiments, will be given by the spatial density of the cores divided by the typical time scale for their motion, assuming approximatively independent core diffusion. The density of cores of size $\xi \sim \ln(1/(1-\rho))/(1-\rho)$, is just the frameable probability around a given origin, $\mu_{\Lambda,\rho}(\mathcal{F}) \sim \Xi^{-d}$. The form of the asymptotic behavior of Ξ in the high density limit was found for any $s < d$, and, for the $d = 2$, $s = 1$ case, the coefficient that enters $\ln \Xi$ was calculated exactly see Section 3.

The typical timescale on which cores move has been discussed in ref. 40. Since all frameable configurations are equiprobable, this is proportional to $\exp(\Delta S)$, the ratio of the number of accessible (frameable) configurations of the core to the number in the most severe bottleneck in the configuration space of the core.[40,53] The worst case scenario for a minimally frameable region of size ℓ would occur if the bottleneck corresponded to a *single* configuration, (the framed one) leading to $\Delta S = S_{\text{total}} \simeq \ln \ell!$ since the total number of frameable configuration is of order $\ell!$. However, as explained in ref. 40 (and to be detailed in ref. 53) the bottleneck is not nearly tight: cores do not have to go through framed configurations in order to rearrange or to move. Numerically we have found that the time scale increases more slowly than exponentially in ℓ and its growth is compatible with an analytic argument for the entropy bottleneck, which yields at least a lower bound. This result is obtained by noting that, in order to fully equilibrate, an optimally frameable square of size

ℓ has to pass through configurations with the nucleus (the three vacancy element, see Fig. 6 and Section 3.2) in a *corner* of the square. Using a transfer matrix technique we obtain for $\ell \times \ell$ optimally frameable squares an entropy difference between configurations with the nucleus in the center (which are typical) and those with the nucleus in the corner asymptotically equal to $\Delta S \approx \Upsilon \sqrt{\ell} + \alpha \ln \ell + C$ with $\Upsilon = 2\sqrt{6 + \sqrt{22}} - 2\sqrt{3} \cong 3.075$ and α computable in principle.[53] This leads, via the observation that the worst blockages are typically when $\ell \sim 1/(1-\rho)$ to a typical timescale for movement of optimally frameable regions

$$\ln \tau_D \sim 1/\sqrt{1-\rho} \tag{56}$$

for the $s=1$ square lattice model. We conclude that the dominant contribution to self-diffusion of a tagged particle, D_S, arises from the low density of mobile cores rather than the long time needed for them to move of the order of their diameter.

The arguments given above can be generalized to any KA models on hypercubic lattices with $s < d$. The conclusion is that, to leading order in $(1-\rho)^{-(d-s)}$, the s-iterated logarithm of the self-diffusion coefficient scales as the s-iterated logarithm of $\mu_{\Lambda,\rho}(\mathcal{F})$. Correspondingly, we expect the typical relaxation times τ to scale with one over the density of cores, i.e. as the inverse of D_S.[16] In particular, thanks to the exact result in Section 3.2, for the $d=2s=1$ model we obtain

$$\lim_{\rho \to 1} (1-\rho) \ln D_S = -\pi^2/9 \tag{57}$$

a prediction which we have successfully verified by numerical simulations.[40] On the other hand, for the case $d=3$, $s=2$, the dependence on density for different relaxation times τ have been considered in refs. 14, 24 and our prediction have been successfully checked, namely data are well fitted by the scaling $\tau \propto \exp \exp C/(1-\rho)$ with C constant.

Note however that there may be very substantial corrections to the leading asymptotic behavior at obtainable densities. Indeed, it is known that there are large corrections to the asymptotic law derived for bootstrap percolation.[49] Therefore, it would be useful to compute sub-leading corrections to all the analytical expressions derived here. First, one should

---

[16]Strictly speaking our results applies directly to D_S. The structural relaxation time could, and very probably will, affected by the slowest regions in the systems which instead are not relevant for the self-diffusion. Hence, we expect a structural relaxation time larger than $1/D_S$, i.e. a decoupling between structural relaxation time and self-diffusion as indeed the numerical results of KA already suggested originally.[11]

take into account the timescale for movement of a core, discussed above. For example in the $d = 2$, $s = 1$ case corrections to $(1 - \rho) \log D_S$ from this will be large – probably of order of $\sqrt{1 - \rho}$. Furthermore, one should take into account corrections to the asymptotic form of the optimal framing probability: we expect these to be negative as occurs for bootstrap percolation where the numerical results for c_∞ [49] correspond to roughly one half of the exact result.[52] (Note that recent progress on the calculation of such corrections for bootstrap percolation has been made.)[54]). A rough cancellation between such a negative correction to the density of the mobile cores, and the positive one arising from the typical timescale, might explain why, in the measured range of densities, $\ln D_S$ seems to be closer to its asymptotic value than is the crossover scale Ξ.

The mechanism that we have identified for the long-time scale dynamics, certainly provides a lower bound on D_S for $\rho \to 1$; this could be probably be proved along similar lines.[53] But how do we know that there is not a faster mechanism which dominates? There are two reasons to strongly believe that there are no faster mechanisms: First, we have proven that the finite size cross-over between irreducible and non-irreducible dynamics takes place exactly when the probability of having at least one core in the lattice crosses from small to large. This strongly suggests that a single core is necessary, as well as sufficient, to relax the system. This is exactly analogous to the behavior for a standard lattice gas in which $D_S \propto (1 - \rho)$ at high density and the change from frozen to unfrozen takes place when there is at least one vacancy in the region. Secondly, rigorous analysis of non-cooperative KA models[41] for which finite clusters of q vacancies can move freely, (such as $s = 1$ on a triangular lattice, for which $q = 2$) show that the self-diffusion coefficient scales as $D_S \propto (1 - \rho)^q$ in the high density limit. The cooperative cases can be understood roughly in terms of a density dependent q: at any fixed density there are no free moving clusters but there is a characteristic sized group of vacancies – a mobile core – that can indeed diffuse since it typically finds enough outer vacancies in each direction (Of course the environment is random and there are some places in which a core cannot enter without changing its size. However these regions would not be important for the self-diffusion coefficient even if they were forever frozen, as happens for diffusion in a disconnected random environment when there is a percolating cluster.). At each density, one needs to have $q \propto \xi(\rho)$, in order to be sure that the diffusion of cores is possible: this yields a mobile core density of the form we have found.

Up to now we have focused on the behavior at high densities, in particular the asymptotic value of relevant quantities in the limit $\rho \to 1$. However, as discussed in more detail in refs. 41, 53 for some lattices,

especially with $s > 1$, the asymptotic behavior will not be relevant except on extremely – perhaps inaccessibly – long-time scales. In practice, much of the slowing down as the density increases could occur before this asymptotic regime. In particular, rapid crossover could occur near an almost transition – sometimes called an *avoided transition*[55] – near an almost-critical density (which would depend on the lattice and the value of s). Such behavior could account, for example, for the apparent power law "vanishing" of the self-diffusion coefficient observed as $\rho \to \bar{\rho} \simeq 0.881$ in simulations of the three-dimensional case with $s = 2$.

A simple argument suggests that such a cross-over might exist.

We again first focus on the two-dimensional case with $s = 1$. As already mentioned in ref. 41, in this case a small (fixed-size) cluster of vacancies can freely diffuse on a second-neighbor-percolating clusters of other vacancies. Therefore,when the vacancy density is above the correspondent percolating threshold, diffusion can occur without substantial cooperativity. But the contribution to the self-diffusion coefficient from this mechanism shrinks to zero as the vacancy percolation threshold is approached from above (from below, in terms of particle density). At higher densities, the mechanism behind diffusion crossesover to the cooperative one discussed in this paper.

For the three-dimensional case with $s = 2$, from the construction in Section 3.3, we expect that the approximate transition seen in numerics may well be related to percolation of surfaces on which the vacancies are nearly connected like those on the surfaces of optimally framed cubes.

The above percolation arguments are only qualitative and we do not expect that the density at which the percolation transition takes place will correspond very well with the density at which the apparent transition takes place. In next section we present a quantitative analysis of an actual transition in KA models. We show that in finite dimensions, apparent transitions with rapid crossovers could arise as "ghosts" of actual dynamical transitions that occur on Bethe lattices – or, equivalently, within the Bethe approximation for real lattices. This suggests a way to study "avoided transitions": by using the Bethe lattice results and perturbing around this "mean-field" limit.

5. KA MODELS ON BETHE LATTICES

Bethe lattices are defined as a infinite loop-free graphs with fixed connectivity $z = k + 1$. The main motivation for studying statistical mechanical models on Bethe lattices is that such "lattices" are often considered to be a good approximation of more realistic lattices, e.g. hypercubic, in the limit of high dimensionality: the Bethe lattice models are then considered

to be a type of "mean field" – or more accurately "uncorrelated field" – approximation. But their tree – like structure enables analytic calculations via recursive procedures.

As we will explain in detail, the behavior of KA models on Bethe lattices is qualitatively different from that on hypercubic lattices obtained in previous sections: on Bethe lattices an ergodic/non-ergodic transition takes place at a non-trivial critical density. Nevertheless, exact results on these lattices, when combined with those for hypercubic lattices, should be useful both for better understanding of the latter, and as background for considering how mean-field-like scenarios for glass transitions might – or might not – be extended to real glasses, or at least to some more realistic models.

5.1. Bethe Lattices

There are subtleties in the definition of Bethe lattices that are important to note. Bethe lattices with connectivity $k+1$ are *locally* identical to the infinite size limit of random "c-regular" graphs with $c = k+1$[56] which are uniformly drawn from the set of graphs with connectivity c for each site with neither multiple edges (no two edges joining the same pair of sites) nor loop-edges that join a site to itself. Since in the limit of large number of sites, with high probability there are no finite loops that go through a given set of vertices, a typical such random graph looks locally (i.e. on any finite length scale) like a Cayley tree with a fixed branching ratio. (Recall that a Cayley tree with connectivity $k+1$ is constructed by taking $k+1$ rooted trees with branching ratio k and connecting all the $k+1$ roots to a new site, which can be considered as the origin.) Nevertheless, for macroscopic properties the presence of loops that exist in even very large random graphs is crucial since it induces geometric frustration and ensures a statistically homogeneous structure which prevents the pathologies that arise for Cayley trees for which a positive fraction of sites are on the boundary which causes extreme sensitivity to boundary conditions. A Bethe lattice corresponds to considering a Cayley tree of size L, focusing on a core of size ℓ around the origin and taking the limit $L \to \infty$ before the limit $\ell \to \infty$, or with the simultaneous limit with both lengths becoming infinite but $\frac{\ell}{L} \to 0$. Note that this is equivalent for models with local dynamics to considering first the limit L to infinity with random initial conditions, and then considering the long-time limit: as such, it is quite physical.

The following analysis holds both for random c-regular graphs with $c = k+1$ and for Bethe lattices, up to the subtleties discussed above.

5.2. Existence of Frozen Phase

KA models on a Bethe lattice with connectivity $k+1$ are defined as in Section 1.3, with $0 < m < k$ and $s = k - m$. As usual, it is convenient to arrange the lattice as a tree with k branches going up from each site and one going down. Before proceeding with a more careful analysis, we first give an argument that on Bethe lattices, in contrast to hypercubic lattices, infinite frozen clusters almost always exist at sufficiently high densities, ρ.

Rough analogs of the infinite networks of frozen fully-occupied slabs that can occur on hypercubic lattices with $s < d$, are fully occupied infinite subtrees with branching ratio $m = k - s$ and hence coordination number $m + 1$: none of the particles on such a fully occupied subtree can move. If a Bethe lattice with coordination number four is arranged with the four bonds coming out of each vertex forming a cross, then all the vertices of a fully occupied three-sub tree (i.e. a subset of the original graph forming a tree with branching ratio equal to three) will appear to have a line going straight through them, and another half line that either terminates at the vertex in a T-junction, or also continues through it. Such trees are thus somewhat similar to a network of bars on a square lattice. In another sense, however, because they have no loops, they are more similar to a *single* two-wide infinitely long solid bar on a square lattice. Because, for $m < k$, the number of potential m-sub trees is exponentially large – in contrast to the number of infinitely long straight slabs on hypercubic lattices – it is natural to expect that a fully occupied frozen subtree will almost always exist at high densities. This can be shown by a simple generalization of the analysis for conventional site percolation on Bethe lattices.[50, 57]

Consider a site, call it i, and the probability, Q', that it is both occupied and is the root of a fully occupied m-subtree on the portion of the Bethe lattice above it. As the existence of such a subtree requires the existence of similar subtrees rooted on at least m of the sites above site i, and these are independent events, each with some probability Q, we can write a simple recursion relation:

$$Q' = \rho \sum_{j=k-s}^{k} Q^j (1 - Q)^{k-j} \binom{k}{j}. \qquad (58)$$

This has the trivial fixed point solution $Q = 0$ for any density, but, above a critical density, ρ_T, it has an additional non-trivial fixed point solution, $Q^*(\rho) > 0$. For the simplest interesting case, $k = 3$, $s = 1$ – loosely approximating the coordination-four square lattice –, one can easily solve the fixed point equation to find $\rho_T = \frac{8}{9}$, a discontinuous jump at $\rho = \rho_T$ to

a non-zero value: $Q^*(\rho_T) = \frac{3}{4}$ and above ρ_T a square-root cusp increase in $Q^*(\rho)$ which eventually saturates at $Q^*(1) = 1$. Other cases with $m \geqslant 2$ behave qualitatively similarly, in particular also exhibiting a discontinuous onset of the fraction of sites in the frozen sub-tree – simply related to Q^* – at a non-trivial critical point at $\rho = \rho_T(k, m)$. For models with $m = 1$, i.e. $s = k - 1$, the existence of an m-subtree is the same as the existence of an infinite fully occupied cluster and the behavior of Q is thus identical to that of conventional percolation: there is a critical point at $\rho_T = \frac{1}{k}$ with Q^* rising linearly from zero as ρ increases further.

What is the significance of these results for KA models? As do other percolation arguments, these provide useful bounds: the existence of an infinite fully occupied m-tree on a k-Bethe lattice, i.e. $Q^* > 0$, is a *sufficient* condition for the existence of an infinite frozen cluster in the corresponding k, m KA model. Thus we can immediately conclude that a frozen phase is possible in these Bethe lattice models at least for $\rho > \rho_T$. We do not, however, yet have a necessary condition for frozen clusters: as can be seen, these can have isolated vacancies within them at least at sites with more than $m + 1$ frozen subtrees nearby.

5.3. Dynamical Transition

We now analyze the behavior with the actual KA constraints by a generalization of the downwards iterative procedure used above.

Consider a particular site and define the following events:

(i) The site is occupied by a particle which can never move up as long as the site below it is occupied; denote by Y the probability of this event.

(ii) The site is *frozen*: occupied by a particle which can never move up *even if* the site below it is empty; denote by F the probability of this event, which is a subset of event (i).

(iii) The site is empty but *blocked* in such a way that particles on lower sites can never move up to the site; denote by B the probability of this event.

By using the tree-like structure and its symmetry under exchange of branches, one can write iterative equations for the (primed) probabilities for the sites in one layer, in terms of the (unprimed) probabilities for the sites in the layer immediately above:

$$Y' = \rho \left(\sum_{j=k-s}^{k} Y^j (1-Y)^{k-j} \binom{k}{j} + \sum_{j=s+1}^{k} B^j Y^{k-j} \binom{k}{j} \right),$$

$$B' = (1-\rho) \sum_{j=k-s+1}^{k} F^j (1-F)^{k-j} \binom{k}{j}, \qquad (59)$$

$$F' = \rho \left(\sum_{j=k-s+1}^{k} Y^j (1-Y)^{k-j} \binom{k}{j} + \sum_{j=s}^{k} B^j Y^{k-j} \binom{k}{j} \right).$$

These can be alternately written for Y in one layer as a function of the three Ys in the three next higher layers.

We are particularly interested in stable fixed points of the iterative equations which correspond to the desired behavior in the interior of the system; the fixed point equations can be reduced to independent polynomial equations, with ρ dependent coefficients, for any one of the Y, B, or F. For ease of notation, except when it might be confusing, we will denote fixed point probabilities simply by Y, F, B and Q.

We have earlier shown that there exists a frozen phase at high densities: in particular for $\rho > \rho_T$ the probability Q is non-zero. Since when the event corresponding to Q occurs, the particle is definitely frozen, we know that $F \geqslant Q$; F non-zero then implies from (59) that both Y and B are also non-zero at high densities.

To show that all the restricted events have zero probability at low densities, it is sufficient to note that Y', F' and B' all depend at most linearly on Y, F, and B (as the other powers in the polynomials are greater than unity), and two of the coefficients are ρ. Thus at sufficiently low densities, Y must decrease on iteration by a factor that is no larger than a multiple of ρ. Thus the only fixed point at low densities is $Y = B = F = 0$.

We have thereby shown that a dynamical phase transition must exist for Bethe lattice KA models with $0 < s < k$. We now show that, except for $s = k - 1$, this transition is discontinuous.

5.3.1. Discontinuity at Transition for $s < k - 1$

For KA models with $s < k - 1$, i.e. $m \geqslant 2$, one can show straightforwardly that the transition is discontinuous. Focus on one site, call it x. A particle on x can move up even if the site below it is occupied, if at most one of the k sites above x and the k^2 sites one level further up are occupied. In such a situation, the marginal event whose probability is Y

does not occur. For the empty sites in the two levels above x, the marginal occupied event does not occur either and the probability of such sites is thus at least $1 - Y$. With all probabilities having their fixed point values, these observations imply that

$$Y \leqslant 1 - (1 - Y)^{k+k^2} - (k + k^2)Y(1 - Y)^{k+k^2-1} . \qquad (60)$$

But this inequality cannot be obtained if Y is positive but small, since for $0 < Y \ll 1$ it would become essentially $1 \leqslant (k + k^2 - 1)(k + k^2)Y$, which cannot hold for small Y. Therefore, the fixed point value of Y cannot go continuously to zero: it must jump to a non-zero value at the critical density, ρ_c.

Note that this argument does not apply for the case $s = k - 1$. This is because, even if all but one of the sites immediately above x are empty, a particle on x can still not move up if the site below it is occupied (the inequality (60) in this case does not have the second term on the right hand side; this invalidates the rest of the argument).

5.3.2. Continuity of Transition for $s = k - 1$

Now consider the most highly constrained non-trivial case: $s = k - 1$. In contrast to the less constrained models, for a particle to be frozen in this case, it need only belong to an infinite cluster of particles with two or more neighbors, i.e. to a percolating cluster in the conventional sense of nearest neighbor percolation. This means that for $m = 1$, the critical density for the KA model should be the same as for percolation, $\rho_c = 1/k$,[57] and the transition will be continuous with Y growing linearly just above ρ_c. By solving Eq. (59) for the simplest such cases, $k = 2$ and $k = 3$, this can be checked directly. More generally, for any $k > 2$ with $s = k - 1$, to quadratic order when it is small, Y' depends only on Y and can be seen to attain a fixed point value $Y \approx \frac{2}{k-1}(\rho - \rho_c)$ just above the transition at $\rho_c = 1/k$; this non-zero Y induces non-zero, but quadratically small, values for both B and F.

5.3.3. Connection to Bootstrap Percolation

As for hypercubic lattices, bootstrap percolation yields bounds for the behavior on Bethe lattices. Before analyzing in detail the character of the dynamical transition, we illustrate this connection which can elucidate the physical mechanism underlying the dynamical transition of KA models.

The relevant bootstrap percolation process is similar to that given earlier for hypercubic lattices (and introduced by KA[11]): From a random

initial configuration with density ρ, remove all the particles that can move according to KA rules and iterate the process until no more particles can be removed. If some particles survive at the end of this procedure, they must be frozen in their initial configuration under the KA dynamics. Define p^B as the probability that at the end of the procedure an infinite particle cluster remains. By the above observation, if $p^B > 0$ the KA model at density ρ is not ergodic. Let ρ_c^B be the critical density, if any, at which a *bootstrap percolation transition* takes place, namely $p^B = 0$ for $\rho < \rho_c^B$ and $p^B > 0$ for $\rho > \rho_c^B$. If there exists such a bootstrap transition, a dynamical transition for the corresponding KA model must also occur and the corresponding critical density satisfies $\rho_c \leqslant \rho_B$. Moreover, a reasonable Ansatz, is that the two transitions and therefore the corresponding critical densities, in fact, *coincide*. In the rest of this section we present an argument supporting this conjecture.

Let x be a site on which a particle is frozen with respect to KA dynamics, i.e. a particle that cannot move on any time scale after the thermodynamic limit has been taken. Than x must have *either*: more than $m = z - s - 1$ neighbors that are occupied and frozen, or, if m or fewer of the neighbors are frozen (and thus the particle on x could potentially move), *all* its unfrozen neighboring sites, either empty or occupied, must themselves have more than m occupied frozen neighbors. If this were not the case, one could move all the unfrozen neighbors out of the way, and then move the putatively frozen particle from site x. Moving the neighbors at the same time is possible in such a situation because the constraints on them are independent since loops that could induce such correlations, do not exist on Bethe lattices. In other words, moving one of the neighboring particles away from a site should not affect the ability of its other neighbors to move and an unfrozen neighboring particle can itself move provided an appropriate set of particles that are further up *its* branch of the tree have moved out of the way. One can repeat the above argument to show that the neighbors of x must each have at least $m - 1 = z - s - 2$ neighbors along their own branches occupied by frozen particles, or else all their unblocked neighbors must themselves have more than $z - s - 1$ frozen neighbors, and so on and so forth. Therefore, the probability $\tilde{P}$ that a given site is occupied by a frozen particle can be expressed in terms of Y and B as

$$\tilde{P} = \rho \left(\sum_{j=k-s+1}^{k+1} Y^j (1-Y)^{k+1-j} \binom{k+1}{j} + \sum_{j=s+1}^{k+1} B^j Y^{k+1-j} \binom{k+1}{j} \right).$$

$$(61)$$

As a consequence in the ergodic phase $Y = B = 0$ and $\tilde{P} = 0$, whereas in the non-ergodic phase Y and B are strictly positive and thus so is $\tilde{P}$.[17]

This result leads to a physical interpretation of the dynamical transition as a "jamming" transition: at ρ_c, an infinite set of blocked particles suddenly appears and concomitantly a breaking of ergodicity occurs.

We have checked the relation between the bootstrap percolation transition and the dynamical transition by performing numerically the bootstrap procedure for the case $k = 3, s = 1$, and verifying that the density above which a cluster of particles remains at the end of the process is compatible with the critical density for the dynamical transition.

5.3.4. Quantitative Results for k = 3, s = 1 and k = 5, s = 2 Models

We now consider in detail the cases $k = 3$, $s = 1$ and $k = 5$, $s = 3$, which mimic, respectively, the non-trivial square lattice model, and the three-dimensional cubic-lattice model originally introduced by KA.

In the case $k = 2$, $s = 1$, Eq. (59) give

$$
\begin{aligned}
Y' &= \rho \left(Y^3 + 3Y^2(1 - Y) + B^3 + 3B^2Y \right), \\
B' &= (1 - \rho)F^3, \\
F' &= \rho(Y + B)^3.
\end{aligned}
\tag{62}
$$

from which one can immediately see that, at a fixed point with $Y > 0$ also $B > 0$ and $F > 0$. Therefore one can study the transition by analyzing the fixed point equations for

$$
G \equiv Y + B
\tag{63}
$$

which can be written in polynomial form:

$$
\begin{aligned}
R(G) = G[-1 + 3\rho G - 2\rho G^2 + v\rho^3 G^8 - 6v\rho^4(G^9 - G^{10}) \\
+ 3v^2\rho^7(G^{17} - G^{18})] = 0.
\end{aligned}
\tag{64}
$$

---

[17]We expect that our derivation of $\tilde{P}$ is correct under the hypothesis that to pick away a particle during the bootstrap procedure, it is not necessary to pick away before so doing, an infinite (i.e. diverging with the system size) number of other particles. This should be roughly equivalent to the hypothesis that an appropriately defined correlation length is finite, a reasonable expectation except at the bootstrap transition point.

By direct analysis one can see that there is a fixed point with $G = 0$ which is stable for *any* density, while above a critical density, ρ_c, a second physical solution appears with positive G; both are stable in this regime. Separating these stable fixed points is an unstable one at an intermediate value of G. As the density decreases to $\rho = \rho_c$, this unstable fixed point annihilates with the non-zero stable fixed point at a saddle-node bifurcation signaled by

$$\frac{\partial R(G, \rho_c)}{\partial G} = 0 \tag{65}$$

at the fixed point.

The values of the critical density ρ_c and critical $G_c \equiv G(\rho_c)$ are:

$$\rho_c \simeq 0.888, \qquad G_c \simeq 0.758 \tag{66}$$

The critical density is strictly less than, although only very slightly so, the critical density $\rho_T = \frac{8}{9}$, of the much simpler two-branching-subtree percolation problem discussed in Section (5.2).

At $\rho = \rho_c$ the value of G jumps discontinuously from the low density value $G = 0$ to G_c and then increases with a square root cusp: $G \approx G_c + C\sqrt{\rho - \rho_c}/\rho_c$, see Fig. 11. Similar behavior obtains for the probabilities $\tilde{P}$ of a site occupied by a frozen particle, as can be obtained from Eqs. (61) and (62).

For the case $k = 5$, $s = 2$, by solving Eqs. (59), a similar transition is found at a slightly higher critical density $\rho_c \simeq 0.915$.

5.3.5. Diverging Time and Length Scales at the Dynamical Transition

Although the dynamical transition in these KA models is discontinuous, there is precursor behavior more characteristic of critical transitions. In this respect, the situation is somewhat analogous to conventional bond percolation on one dimensional lattices with connection probability between any two points proportional to the inverse square of the distance between them.[58]

Indeed from the discussion in the previous subsection, an interpretation of the mixed nature of the dynamical transition of Bethe lattice KA models is suggested: the dense cluster of frozen particles that arises immediately at $\rho = \rho_c$ contains a finite fraction of the particles and it is, at the same time, *fragile* in a way similar to incipient infinite clusters at conventional critical percolation. This fragility implies that by removing a tiny,

but carefully chosen, fraction of the particles, the frozen cluster can be "melted" and will disappear. Associated with this fragility is a correlation length that diverges as $\rho \to \rho_c$ from above. The form of the divergence, $\sim (\rho - \rho_c)^{-\frac{1}{2}}$ is controlled by the "rate" – in tree levels – of approach of the iterated probabilities to the fixed point. Physically, this correlation length is the (chemical) distance beyond which it is unlikely to have to move vacancies in order for a given particle to be moved.

More significant than the long length scales that appear near the critical density, are the corresponding dynamical effects. In particular, we expect a diverging time scale as ρ_c is approached from below. Unfortunately, our analytic methods, while they take into account the dynamical constraints, cannot directly be used to compute the dynamical correlations of primary interest. At this point, we resort to numerical simulations to study these and other properties of the Bethe lattice models.

Before turning to the numerics, we note that the behavior on Cayley trees, because of their boundaries which account for a positive fraction of the volume, might exhibit different phase diagrams depending on the choice of boundary conditions.

5.4. Dynamics and Numerical Simulations

In order to understand in more detail the character of the dynamical transition, we have performed numerical simulations of KA dynamics for the $k=3$, $s=1$, model on a random c-regular graph of $N=10^4$ sites with coordination number $k+1=4$.

In particular we have computed the local density–density dynamic auto-correlation function $C(t)$ and the corresponding dynamical susceptibility $\Psi(t)$:

$$C(t) = \frac{1}{N} \sum_{i=1}^{N} \frac{\langle n_i(t) n_i(0) \rangle - \rho^2}{\rho - \rho^2},$$

$$\chi_4(t) = N \left\langle \left(\frac{1}{N} \sum_{i=1}^{N} \frac{n_i(t) n_i(0) - \rho^2}{\rho - \rho^2} - C(t) \right)^2 \right\rangle,$$

where $\langle \ \rangle$ denotes an average over the Bernoulli product measure at density ρ for the choice of the initial configuration at over the Montecarlo dynamics. The dynamical susceptibility $\chi_4(t)$ (and its generalization) has been introduced in ref. 59 and is currently used[7,24] to detect a growing dynamical correlation length in simulations of glass-forming liquids.
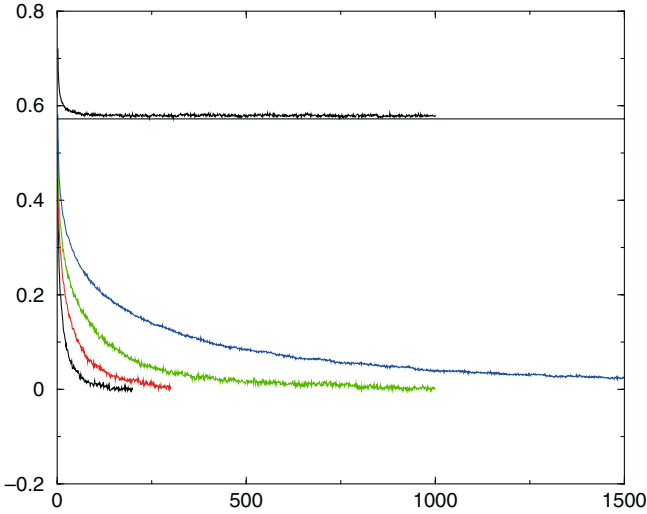
Fig. 10.   color online. Dynamic autocorrelation function $C(t)$ as a function of time for densities 0.85, 0.86, 0.87, 0.875, 0.9 (from down to up) on a 10,000-site approximation to a Bethe lattice with coordination number $k+1=4$ and single-vacancy assisted dynamics. The dynamical transition is clearly evident between the densities 0.875 and 0.9. The straight line is the value of the Edwards–Anderson order-parameter obtained by the approximation discussed in the text.

The results for $C(t)$, plotted in Fig. 10, show that the equilibration time grows and seems to diverge at the critical density found from the quasistatic analytical calculations (see Eq. (66)). Indeed, for $\rho < \rho_c - \Delta$, $C(t)$ tends to zero at long times but with a characteristic decay time that increases at higher densities. Here Δ, the precision obtained for ρ_c, is 0.0075. For $\rho < \rho_c + \Delta$, $C(t)$ no longer appears to decay to zero but seems to approach a non-zero plateau whose magnitude it is natural to call an Edwards–Anderson parameter by analogy with spin glasses. Since at the critical density there should be $N\tilde{P}(\rho_c)$ frozen particles, the value of the Edwards–Anderson parameter $q_{EA} \equiv \lim_{t \to \infty} \lim_{N \to \infty} C(t)$ has two contributions coming from sites that are occupied respectively by a frozen particle or by a vacancy that can never move. These can be computed exactly from the quasi-static computation developed in the previous section. However there is a third contribution that corresponds to

$$\lim_{t \to \infty} \frac{1}{N} \sum_{i=1}^{N'} \frac{\langle n_i(t) n_i(0) \rangle - \rho^2}{\rho - \rho^2},$$
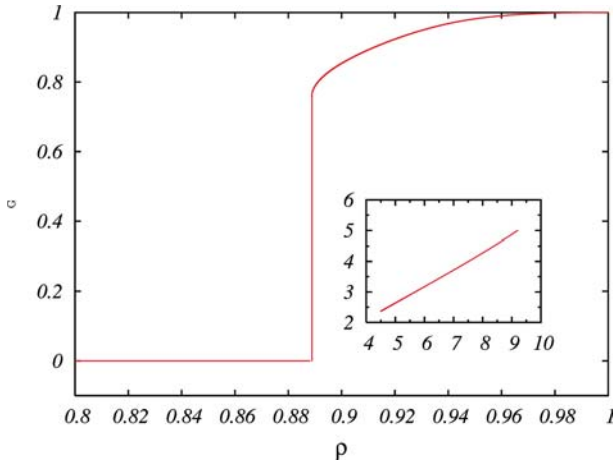
Fig. 11. color online. The probability, G (defined in the text) as a function of density for $k=3$, $s=1$ Bethe lattice as obtained from the stable solution of Eq. (64). In the inset $log(G - G_c)$ is shown as a function of $log(\rho - \rho_c)$ in the vicinity of ρ_c showing the square root dependence.

where the index $i=1,\ldots,N'$ runs only over the sites whose occupation number changes during the dynamics (i.e. they are not occupied by vacancies or frozen particles). This contribution to q_{EA} is more cumbersome to compute. In this paper we just give a rough approximation which consists of assuming that the long-time limit of $\langle n_i(t)n_i(0)\rangle$ on these sites – which consist of many small disconnected clusters – is equal to the density of particles within the full set of N' dynamic sites. This can be computed from the quasi-static analysis developed in the previous section. Comparison with numerics shows that this approximation works rather well (see e.g. Fig. 10).

A dynamical quantity that can be computed exactly is the long-time limit of the *persistence function*: the probability that the occupation variable of a given sites has not changed from its initial value for an interval of time t. The long-time plateau of this, by definition, is equal to the fraction of sites that are occupied by either a frozen particle or by a vacancy that can never move.

Plots of the dynamical susceptibility, $\chi_4(t)$, found in the simulations are shown in Fig. 12 for various densities: these appear consistent with a divergence at the critical density. More precisely both the height of the peak and the characteristic time scales at which this occurs, appear to diverge at ρ_c.
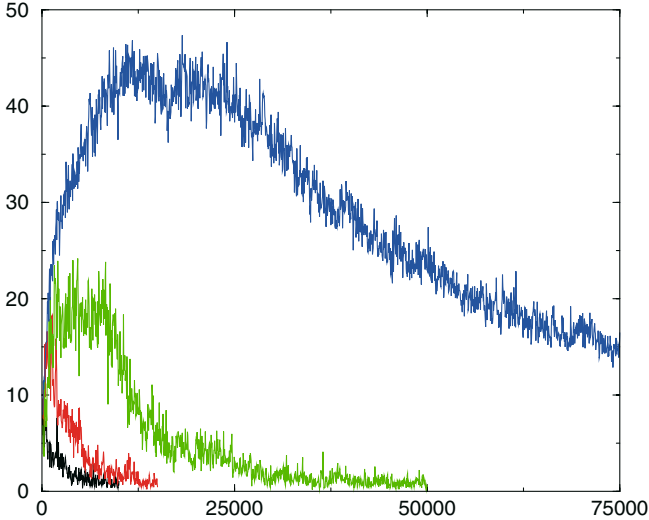
Fig. 12.   color online. Dynamical susceptibility $\chi_4(t)$ as a function of time for densities $0.85, 0.86, 0.87, 0.875$ (from down to up) on a 10,000-site approximation to a Bethe lattice with coordination number $k+1 = 4$ and single-vacancy assisted dynamics.

5.4.1. Configurational Entropy

If phase space breaks into a sufficiently large number of different ergodic components, some of the equilibrium *entropy density* will be associated with the logarithm of the number, $\mathcal{N}_e$, of distinct components:

$$S_c(\rho) = \ln \mathcal{N}_e / V \tag{67}$$

where V is the total number of sites. This is referred to in the glass literature as the *configurational entropy*.[18]

For KA models on Bethe lattices one can find a lower bound for the configurational entropy by observing that all the configurations belonging to the same ergodic component must have the same cluster of frozen particles, therefore $\mathcal{N}_e$ is at least as large as the number of different sets of

---

[18]This terminology is somewhat misleading since in general statistical mechanics "configurational entropy" refers to the sum over all configurations (after having integrated out the momenta). For glasses, its meaning is the contribution to the entropy density coming from the large number of different ergodic components. The other contribution to the entropy is related to the number of configurations within the given ergodic component.

frozen particles, $\mathcal{N}_f$, which has an entropy density,

$$S^f(\rho, \rho_F) = \frac{1}{V} \ln \mathcal{N}_f. \tag{68}$$

Furthermore, the entropy of the non-frozen sites, $S^i(\rho, \rho_F)$, can be bounded above by the number of ways of putting $V\rho - V\rho_F$ particles on $V - V\rho_B$ sites, where ρ_F is the density of frozen particles at total density ρ:

$$S^i(\rho, \rho_B) \leqslant (1 - \rho_B) \ln(1 - \rho_B) - (\rho - \rho_B) \ln(\rho - \rho_B) - (1 - \rho) \ln(1 - \rho). \tag{69}$$

Since the total entropy density,

$$S(\rho) = -\rho \ln \rho - (1 - \rho) \ln(1 - \rho) = \left(S^f(\rho, \tilde{\rho}_F) + S^i(\rho) \right), \tag{70}$$

and we know that $\tilde{\rho}_F = \tilde{P}$ that was computed earlier, see Eq. (61), we obtain a lower bound for the configurational entropy

$$S^c(\rho) \geqslant S^f(\rho, \tilde{P}) \geqslant -\rho \ln \rho - (1 - \tilde{P}) \ln(1 - \tilde{P}) + (\rho - \tilde{P}) \ln(\rho - \tilde{P}). \tag{71}$$

In Fig. 13 this lower bound is plotted as a function of density for the case $k = 3$, $s = 1$. Note that, among other factors, we have ignored in this estimate the existence of empty but blocked sites: the effect of these will be to lower the entropy of the unfrozen particles.

In conclusion, our results from lower bounds and analytical and numerical analysis of the dynamical transition support the expectation that the configurational entropy jumps form zero to a non-zero finite value precisely at ρ_c. For $\rho > \rho_c$, the configurational entropy decreases with the decreasing vacancy density and overall entropy; it vanishes at $\rho = 1$.

5.5. Bethe Lattices with Loops

In order to investigate whether the absence of loops is the essential reason for the existence of a phase transition on Bethe lattices, we briefly consider structures that are tree-like on large scales, but do have loops.

Specifically, consider the rooted tree composed of triangles with one vertex pointing downwards and the other two vertices each being the bottom vertex of another triangle and hence the root of a tree. Then define a Bethe lattice with triangular loops as the graph obtained by taking two
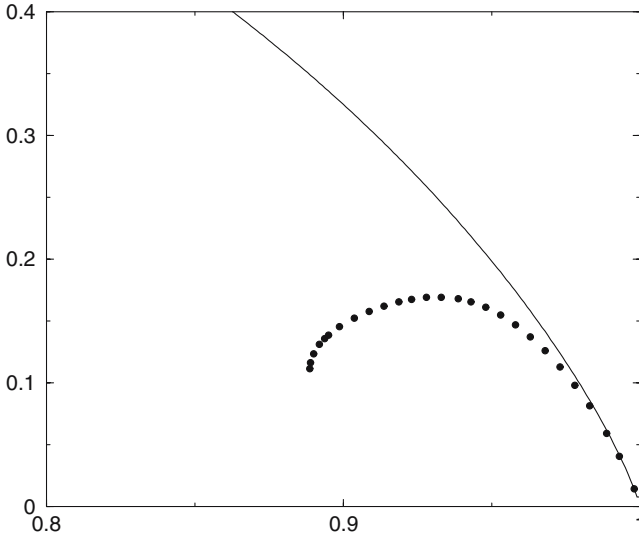
Fig. 13.   Lower bound, $S^b(\rho)$, on the configurational entropy – logarithm of the number of frozen configurations per site – as a function of density for the $k=3$, $s=1$. Bethe lattice is indicated by the dotted line; this bound is obtained from Eqs. (71) and numerical solution of Eqs. (61), (62). Below the critical density $\rho_c \simeq 0.888$, the lower bound jumps to zero. The straight line is the equilibrium entropy.
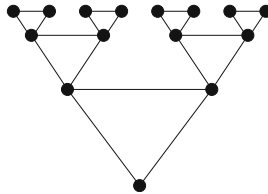

Fig. 14.   A branch of a Bethe lattice with triangular loops.

such lattices and merging the free vertices of the two roots (see Fig. 14). The coordination number of such a tree is $z=4$ and the branching ratio $k=2$. This is an example of a cactus, or Husimi, tree[60] with primary clusters of three vertices and three branches departing from each cluster.

Consider the KA model with $s=1$ on the triangular tree defined above. It is useful to focus on the set $\mathcal{E}_i$ of configurations of the subtree rooted at triangle i, such that the bottom vertex is occupied and a vacancy cannot be brought down to it without using vacancies below it on the tree. Let P be the probability of such an event. If a configuration, η has all three sites of triangle i occupied and all of the subtrees rooted on trian-

gles two levels up from i, $i^1, \ldots, i^4$, have configurations $\in \mathcal{E}_i^j$, then the configuration of the subtree rooted at triangle i belongs to $\mathcal{E}_i$. The same is true for any configuration, η, that has the three sites of i all occupied, and $\eta \in \mathcal{E}_{\bar{i}j}$ for three of the four subtrees rooted at the $\{i^j\}$. Therefore

$$P \geqslant f(P) = \rho^3 \left(P^4 + 4P^3(1-P) \right). \tag{72}$$

Since $P = 1$ is a fixed point of $P' = f(P)$ when $\rho = 1$, at sufficiently large density there exists a $\bar{P} > 0$ such that $f(\bar{P}) = \bar{P}$. If one iterates down the tree for actual Ps, then the inequality (72) implies that, starting from an initial condition $P_0 = \bar{P} + \epsilon > \bar{P}$, all the subsequent P's, $P_1, P_2, \ldots$, will be larger than $\bar{P}$. Indeed, since the $f(x)$ is monotonically increasing in $0 < x < 1$, $P_1 \geqslant f(\bar{P} + \epsilon) > f(\bar{P}) = \bar{P}$ and the same is true at any subsequent step. Therefore, the full fixed point must have $P^* > \bar{P} > 0$. Thus for sufficiently large ρ, $P^*(\rho)$ will be non-zero and the system in a frozen phase. It immediately follows that the density of frozen particles, $\tilde{P}$ is non-zero.

A generalization of the argument in Section 5.2 allows one to prove that there exists a transition at a non-zero density from a regime where $P = 0$ to a region where P is positive. Let $\overline{\mathcal{E}_\rangle}$ be the complement of $\mathcal{E}_i$ defined above. A configuration is definitely in $\overline{\mathcal{E}_i}$ if the four branches rooted at the four triangles two levels up from i are in $\overline{\mathcal{E}_{ij}}$. The same is true if just three of them are in $\overline{\mathcal{E}_{ij}}$ and furthermore one can have or bring vacancies in the highest sites of the triangle which is just above the site which is in the same triangle of the site that cannot have the vacancy. This sufficient condition for $\overline{\mathcal{E}_\rangle}$ yields and upper bound on P:

$$P \leqslant 1 - (1-P)^4 - 4P(1-P)^4, \tag{73}$$

which implies – as in Section 5.3.1 – that P has a *jump* from zero to a non-zero value at the critical density.

The arguments given above can be extended to KA models with any constraint parameter, s, on generalized Bethe lattices with n-polygonal loops for any n, i.e. trees composed of polygons of n vertices, each which is also a vertex of another polygon. To prove the existence of the transition, it is sufficient to consider the set of configurations $\mathcal{E}_i$ such that a vacancy is not and cannot be brought down to the bottom vertex i without using vacancies below. By the same argument as above, we can bound the probability P of such an event by

$$P \geqslant \rho^n \left(P^{(n-1)^2} + (n-1)^2 P^{(n-1)^2-1}(1-P) \right) \tag{74}$$

which implies again that $P > 0$ for sufficiently high density. Generalizing the procedure used for the triangular tree one obtains an bound in the opposite direction:

$$P \leqslant 1 - (1-P)^{(n-1)^2} - (n-1)^2 P^{(n-1)^2-1}(1-P) \tag{75}$$

which implies, as above, that the transition is discontinuous.

Another class of Bethe-like lattices with loops is also instructive to analyze. Consider, as an example, starting with normal Bethe lattice with connectivity four and replacing each site by a square lattice $\Lambda \in \mathbb{Z}^2$ of linear size L connected to to other squares along its edges (see Fig. 15). If we arrange the lattice as a tree with one branch pointing down from each vertex, the "upwards" branches from a square consist of an upwards extension of the lower branch and side branches emerging perpendicularly from the other two sides. Locally, this looks like a square lattice except at the corners: the corner sites still have four neighbors – albeit on three other squares – but have eight second neighbors that are each on separate "sheets" in contrast to the four second neighbors on a regular square lattice each of which can be reached in two distinct ways.

Drawing the tree of squares as described above immediately implies that for the $s = 1$ KA model on which we will focus, there exist infinite networks of frozen particles. As for the normal square lattice, these consist of two-wide fully occupied bars, each either extending to a faraway boundary, or beginning and terminating at T-junctions with other such bars. But such a network, because of the large scale topology of the Bethe lattice, is very different from its real-square-lattice counterpart. It is still very fragile but there are so many potential T-junctions, which are independent of each other if the bars emerging from them go onto different branches, that such a frozen network exists almost surely at sufficiently high densities. The reason for this is simple: consider a vertical bar coming into

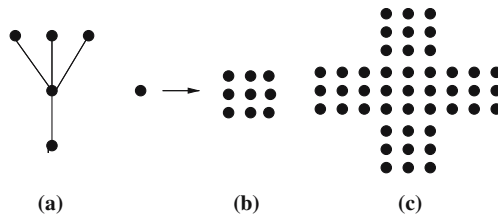(a)   (b)   (c)

Fig. 15. Starting from a Bethe lattice of connectivity $k+1$ (a) we substitute each site with a square of side L thus obtaining a Bethe lattice with loops (c). In the figure we have chosen $k+1=4$ and $L=3$.

a square, i, from below. There are at least two possibilities: the bar can continue through i and into the square above it, or it can end at a T-junction with a bar that extends horizontally into *both* of the other two neighboring squares of i. Since the probabilities, T, that the extensions into each of the three neighboring squares exist and are themselves part of infinite frozen networks on their own sub-trees – i.e., excluding square i – are independent of each other, one can bound from below the probability that square i has a bar rising vertically from its lower boundary and either extending through the top boundary or ending at a T-junction with a bar that extends into the two side boundaries, in terms of T and ρ. As in cases we have already analyzed, this can be used to show that there must be an infinite frozen network at sufficiently high densities. One can likewise show that the transition to the frozen phase will be discontinuous.

To show that the transition on this Bethe lattice of squares is discontinuous, it is useful to focus on the framing by vacancies of individual squares, in the sense used for the conventional square lattice. Consider the event that, without taking advantage of possible vacancies in the square below I, one cannot frame the configuration in I, i.e. reach a configuration with all the boundary sites of I empty. Call X the probability of such an event. If, without using the square i, the three squares left, right and above I can all framed, or if either the above and left or the above and right squares can be framed, or if the left and right squares can be framed and in the square I the first row is empty and all the others are occupied then the square I can definitely be framed. These possibilities are sufficient, but not necessary. Therefore

$$X \leqslant 1 - (1-X)^3 - [2 + \rho^{L^2-L}(1-\rho)^L]X(1-X)^2 \qquad (76)$$

which is incompatible with a continuous transition by an argument similar to that used for other Bethe lattices.

In general, the existence of finite loops on these decorated Bethe lattices, makes the motion of particles less restricted that on a regular Bethe lattice. Indeed, there will be configurations in which two or more vacancies can be ejected from one branch up into another, and by making use of these, trigger the potential ejection of a larger number of vacancies down from the second branch. This process can depend on configurations arbitrarily far up in the two branches. Such ejected vacancies could in principle extend their influence arbitrarily further down the tree and render all particles mobile, even when the density is above the critical value for the loopless Bethe lattice. But the above results show that for low enough vacancy concentration this will not occur: the system will be in a partially frozen state like that of the

simple Bethe lattices. The above picture does, however, suggest a route to estimating the critical density as a function of L.

The trees-of-squares we have been studying interpolate between simple Bethe lattices, for $L = 1$, and a full square lattice for $L = \infty$. Therefore on the trees-of-squares, in the limit $L \to \infty$ the critical density, $\rho_c(L)$ should go to one. But *how* does it approach one? From scaling arguments, one would guess that the framing probabilities on the tree will be functions of the ratio of L to one of the characteristic lengths of the infinite square system: i.e. functions of either $L/\xi(\rho)$, or $L/\Xi(\rho)$. Naively, one might expect that the behavior would be controlled by the large crossover length, which determines the spatial density, $1/\Xi(\rho)^2$, of mobile cores and thus the probability that squares of size L are frameable. However, this ignores the effects of possible help from vacancies moved from other squares and the correct behavior can be seen as follows. Consider one of the L by L squares that *can* be framed by vacancies. The probability that this framing can be continued all the way through a given one of its neighboring squares to make an $L \times 2L$ framed rectangle, is of order $[a(1-\rho)L]^L$ with an order-one coefficient a. This will be substantial as long as $\xi(\rho) > L$ – in spite of the fact that the probability the original square was frameable is very small unless $L \sim \Xi(\rho)$. The crucial observation that leads to a scaling with ξ, is a consequence of the tree structure: once the neighbor square of i has been framed together with i, as above, each of the three other neighbors of this neighbor can potentially join the frame as there already exist complete rows of vacancies along one of their sides from which the framing can be extended. Since any of these squares that joins the frame gives rises to another three potential squares that might join as well, if the original square frame can be extended out in several directions to make a small frameable tree, it become likely that it can be extended much further, indeed, to infinity. Thus the crucial condition for extending the framing to infinity is that there be a substantial probability of a frame around one square being extendable across *one* of its neighboring squares – even when the probability that a single square is frameable on its own is beery small.

We conclude that the critical density, $\rho_c(L)$ for the $s = 1$ KA model on a tree of $L \times L$ squares, will be given by

$$\xi(\rho_c) = bL \qquad (77)$$

with some order-one coefficient b. As $\xi \sim \ln[1/(1-\rho)]/(1-\rho)$ for high densities, this yields

$$\rho_c(L) \approx 1 - \frac{B \ln L}{L} \qquad (78)$$

with some coefficient B. Note that this form is the same as that suggested by the argument given above for the appearance of an infinite network of bars of frozen particles, since the probability of a two-wide fully occupied bar crossing a square is of order $L\rho^{2L}$ which is of order one at $\rho_{\rm c}(L)$.

6. FREDRICKSON ANDERSEN MODEL

The FA model is a spin model with kinetically constrained dynamics that is similar to the KA model but without a conservation law: roughly speaking KA models are FA models with dynamics that conserves the number of particles. Some of the results discussed previously for KA models have been previously obtained for FA models:[9,29,44] for example irreducibility on some hypercubic lattices for the non-trivial range of the constraint parameter. However, there are important results, like the absence of a ergodic/non-ergodic transition, that have not been proven previously, as well others, such as the dependence of the relaxation time scale on density, that can be made sharper. In the following we briefly discuss how these new results on FA models can be obtained using the same techniques that we have developed for KA models.

6.1. Definition of the Model

Let Λ be an hypercubic d–dimensional lattice and f an integer parameter in the range $0,\dots,2d$. The FA model[29] is a facilitated Ising model with "occupation" variables $\eta_x \in \{0,1\}$ – configuration space $\Omega_\Lambda = \{0,1\}^{|\Lambda|}$. The FA model is conventionally defined in terms of spin variables; we use occupation variables to make comparisons with KA models more natural. The occupation variables can "flip" with rate

$$c_x(\eta) := \begin{cases} 0 & \text{if } n_x(\eta) \leqslant f \\ \min\left(1, \exp - \frac{\Delta H}{T}\right) & \text{otherwise,} \end{cases} \tag{79}$$

where

$$n_x(\eta) := \sum_{\substack{y \in \Lambda \\ |x-y|=1}} (1 - \eta_y), \tag{80}$$

i.e. n_x is the number of empty neighbors of x and the change in energy $\Delta H = H(\eta^x) - H(\eta)$ comes from the non-interacting Hamiltonian

$$H = -\frac{h}{2} \sum_x \eta_x \tag{81}$$

with h a positive coefficient that determines the fraction of occupied sites in equilibrium. These rates satisfy detailed balance with respect to the trivial equilibrium product measure

$$\mu_{\Lambda,T}(\eta) = \prod_{x \in \Lambda} \left(\frac{\exp(\beta h)}{1 + \exp(\beta h)} \right)^{\eta_x} \left(\frac{1}{1 + \exp(\beta h)} \right)^{1 - \eta_x} \tag{82}$$

with $\beta = 1/T$: this corresponds to Bernoulli measure with density

$$\rho = \exp(\beta h)/(1 + \exp(\beta h)). \tag{83}$$

In contrast to KA models, $\sum_{x \in \Lambda} \eta_x$ is not conserved in FA models: a "flip" at a single site corresponds to the birth or death of a particle.

In the unrestricted case $f = 0$, the FA dynamics is simply Glauber dynamics for uncoupled Ising spins in a magnetic field: occupied sites corresponding to up spins and vacant sites to down spins. But for positive f, a site can change only if at least f of its nearest neighbors are empty (i.e. their occupation variables equal zero), we refer to empty sites as *facilitating* and to f as the *facilitation parameter*. For $f > d$, fully occupied hypercubes will be frozen. We thus restrict consideration to $1 \leqslant f \leqslant d$. Since energy favors occupied sites, in the low temperature regime most potential flips will not be allowed. Therefore we expect dynamics to be slow in this regime, as for the high density regime of KA models. On finite lattices, as for KA models, there is not a unique invariant measure: there exist blocked configurations and the FA dynamics are not ergodic. But irreducibility in the thermodynamic limit for $f \leqslant d$ has been proved for two and three – dimensional hypercubic lattice FA models, [44,51,61] (see ref. 9 for a review).

There is considerable similarity between KA and FA models: in the former, a particle cannot move if it has more than m occupied neighbors; in the latter it cannot flip to vacant if it has more than $2d - f$ occupied neighbors. Thus f plays a similar role to $2d - m$, or, equivalently, to $s + 1$, with s the KA model parameter that restricts a vacancy from moving if it has fewer than s neighboring vacancies. In addition to their conservation law, the KA models differ from FA models because of their restrictions on the neighbors of two sites (the initial and final sites for the jumping particle) for each possible move.

6.2. Irreducibility and Ergodicity

The presence or absence of frozen configurations in FA models is simply related to bootstrap percolation. Consider a configuration of

occupation variables and perform a boostrap procedure by removing at each step all particles that have at least f empty neighbors. If, at the end of this procedure no particles remain, the initial configuration belongs to the irreducible component that contains the totally empty configuration (called the high temperature partition by FA). This is exactly conventional bootstrap percolation. But all the "moves" made in this bootstrap procedure are allowed in the corresponding FA model. Therefore, using the results for the absence of an unpercolated phase for bootstrap percolation,[51,61] one can immediately conclude that in the thermodynamic limit irreducibility holds for FA models at any temperature as long as $f \leqslant d$. In contrast to KA models for which bootstrap moves would not be allowed, for FA models bootstrap results are sufficient to conclude irreducibility in the thermodynamic limit. The result proven for the two and three-dimensional cases[44] is trivial to generalize to higher dimensional cases using the bootstrap percolation results.[62] Furthermore, the crossover length $L^B(\rho)$ that characterizes the bootstrap procedure is not only a lower bound for the crossover length, $\Xi(T)$ of FA models, (as was the case for KA models) but coincides with it under the change of variables $\rho \rightarrow \exp(\beta h)/(1 + \exp(\beta h))$.

As we explained previously, irreducibility in the thermodynamic limit is not a sufficient condition for ergodicity, which is the physically interesting property for dynamics. However, ergodicity can be proven as in Section 2.5, using again irreducibility and the product form of equilibrium measure.

6.2.1. Transition on Bethe Lattices

On Bethe lattices, FA models with positive f displays a dynamical transition and aging dynamics.[63,64] This is a natural expectation that follows from the bootstrap percolation transition on Bethe lattices: our analysis for the KA model – part of which involved removing particles as allowed in FA models – leads, in the FA case on a Bethe lattice, to exactly the same bootstrap percolation equations as in ref. 50. We will not discuss further Bethe lattice FA models.

6.3. Dynamics

We now turn to the dynamics for FA models on hypercubic d-dimensional lattices.

It is well known from previous results and simulations that the behavior is strikingly different for the case $f = 1$ than for larger f.[5,9,29] With $f = 1$, a single vacancy can facilitate the flip of any of its neighbors,

therefore relaxation does not require cooperative processes and time scales are proportional to the density of vacancies, as confirmed by numerics. This least-restricted FA model is loosely analogous to the $s-1$ KA models normal hard core lattice gas (which would correspond to KA with $s=0$) for which a single vacancy can freely move in an otherwise totally filled lattice: in the FA case, a vacancy can "move" by flipping a neighboring occupied site, and then flipping to occupied at the original site. Nevertheless, this analogy cannot be take too far: interesting – although not cooperative – behavior does exist for $f=1$ FA models. Indeed it has been shown in ref. 19 that in dimension less than *four* vacancies cannot be considered as independently diffusing defects (in contrast to the trivial KA model in which single vacancies can move). The interaction between vacancies, in particular their creation and annihilation, lead to a reaction-diffusion process that belongs to the same universality class as directed percolation in three dimensions.

For more restricted FA models with the facilitating parameter $f>1$ neither a single facilitating vacancy, nor a finite cluster of them, can enable all the other sites to flip if these are initially all occupied: as for KA models, a finite vacancy cluster can never breakthrough a slab that is infinite in $2d-f+1$ directions and of width two in the other $f-1$ directions. Hence, cooperative processes must be involved in the low temperature relaxation of these FA models. The nature of the cooperative mechanism that causes equilibration has been conjectured by Reiter.[44] It is very similar to the one we discussed for the KA model in ref. 40 with the correspondence $f \to s+1$.

Consider for simplicity the two-dimensional case with $f=2$ at temperature T and focus on regions of an infinite lattice that are frameable – in the KA sense with $s=1$ (see Section 2.1) – out to linear size $\xi(\rho)$, with $\rho(T)$ defined in (82) and ξ as in (9). These we refer to as mobile cores.[40] It is easy to check that using moves allowed by FA rules every occupation variable inside the core can be changed to zero. On a typical line segment of length $\xi(\rho)$ outside the special core regions, there is likely to be at least one vacancy. The existence of such vacancies around most places a core could be, ensure that a single core can diffuse through typical regions of the system – and eventually everywhere. Reiter conjectured that the diffusion of these *macro-defects* is the dominant mechanism for relaxation in the low temperature regime of FA models. From knowledge of the temperature dependence of ξ and of the spatial density of mobile cores, ρ_D,– both given by those of the corresponding KA model at the same vacancy density, ρ, see Section 6.1 – together with the characteristic time τ_D, within a core, one can make a prediction for the temperature dependence of the overall relaxation time. Neglecting, as for KA models,

the interactions, annihilation and creation of the macro-defects, the bulk relaxation time is ref. 40:

$$\tau \approx \frac{\tau_D}{\rho_D}. \tag{84}$$

This is the time after which typical sites will be changed because a macro-defect has passed by.

Reiter assumed that the typical timescale τ_D for the motion of a *macro–defect* of size l grows as $\exp Kl$ with K a positive constant. However, we have found – analytically and numerically – that this is not the case for the KA model: τ_D increases more slowly with l as $\exp K\sqrt{l}^{(40)}$ (see also Section 4). This result should carry over to the FA case since it is easier for a *macro-defect* to move with FA dynamics than with KA dynamics, yet the dynamics within a core is dominated by entropic barriers[40] which will be the same for both models. As a consequence of the sub-exponential slowing down within a core, the leading contribution to the structural relaxation timescale τ is given by the density of defects and not by their timescale to move. The same argument should hold for any d, $1 < f \leqslant d$ giving $\tau \propto \rho_D \simeq 1/\Xi_{d,f-1}(\rho(T))^d$, where $\Xi_{d,f-1}(\rho)$ is the cross-over length of the corresponding KA model and $\rho(T)$ is the equilibrium density of vacancies at temperature T, see Eq. (83). For the case $d=2$, $f=2$, we thus have the exact leading low temperature behavior of $\log \tau$:

$$\tau \simeq \exp -\frac{2c_\infty}{1-\rho}, \tag{85}$$

where $2c_\infty \simeq 1.1$ (see Eq. (54)). Numerical simulations on a square lattice agree well with the above prediction.[26] However one has to be careful because of strong finite size effects as discussed for the KA case. And there is another complication that might arise in the FA case: the fact that the independent defect diffusion assumption fails in the $f=1$ case for $d<4$,[19] suggests it will also for larger f. However if, as for $f=1$, the fluctuations in $d<4$ just change (slightly) the dynamical exponent that relates time and length, then the scaling of τ with the density for the $d=2$, $f=2$ case would be the same as in (85) but perhaps with a (slightly) renormalized constant c_∞. (In the more cooperative cases for which there are at least two iterated exponentials, a change in the dynamical exponent may not even change the leading asymptotic behavior of the relaxation time, but this needs a more careful investigation.)

7. CONCLUSIONS

We have analyzed in this paper a class of kinetically constrained lattice models which had previously been studied primarily via numerical simulations. For the KA models on hypercubic lattices, we have found that the behavior in infinite systems, in contrast to what was suggested by the simulations, is simple: either the system is non-ergodic for all densities because of the existence of finite frozen clusters, or it is ergodic at all densities. Nevertheless, in the latter cases dynamics at high densities is intrinsically collective and thus non-trivial. We found that there are two length scales that characterize this collective dynamics: The smaller one, ξ, is the linear dimension of a minimal set of vacancies that is *typically* mobile in a system of density ρ; such regions of size ξ^d are the mobile cores whose motion allows rearrangements of other regions. The longer length scale, Ξ, is the typical spacing between mobile cores. Therefore Ξ is the crossover length that determines whether finite-size systems will typically be almost ergodic, with one irreducible set dominating configuration space, or have their configuration space broken up into many large sets. Furthermore, the same length controls the high density behavior of relaxation times, which scale as the density of mobile cores, therefore as $1/\Xi^d$. The manner in which these lengths diverge as the density approaches unity depends on the dimension and the constraint parameter, s. But, although we have not discussed it thus far, there is considerable universality.

7.1. Universality

For simple lattices other than hypercubic, the behavior can be guessed by analogy with the hypercubic cases.

If there are no finite frozen clusters, but infinite frozen configurations do exist, then the minimum dimension of frozen structures will determine the behavior. If the minimal frozen structures are $d - 1$ dimensional, then the frames of vacancies used to show irreducibility will be one-dimensional and the core size will grow with density as,

$$\xi(\rho) \sim \frac{\ln[1/(1-\rho)]}{(1-\rho)^{p/(d-1)}}, \tag{86}$$

where p is the number of nearest neighbor vacancies needed on each side to enable a frame to grow. The crossover scale grows roughly as $\Xi \sim e^\xi$. This least-restricted collective behavior obtains for $s = 1$ on hypercubic lattices in all dimensions, and also for, e.g., two-dimensional triangular lattices with $s = 2$ ($s = 1$ has mobile pairs of vacancies); and three-dimensional

fcc lattices (close-packed) with $s = 3$ ($s = 1$ or 2 models have small mobile clusters of vacancies). In all these cases $p = 1$.

If the smallest frozen structures are $d - 2$ dimensional, framing by two-dimensional planes is needed: this gives rise to

$$\xi \sim \exp\left(\frac{c}{(1-\rho)^{p/(d-2)}} \right). \tag{87}$$

This form cannot occur in two dimensions. In three dimensions, it obtains for cubic-lattices with $s = 2$, as well as for fcc lattices, for $s = 4$ and $s = 5$, these two cases only differing by the numerical coefficient.

In three dimensions, the above are the only possibilities in the same general class that we have been studying, but in higher dimensions, the iterated exponential forms of (35) can occur. As we have shown, on Bethe lattices – expected to be loosely related to some high dimensional limit – an actual dynamical transition at a non-trivial density, ρ_c, does occur for KA models.

This immediately suggests a crucial question: Do some finite dimensional models exist with this type of dynamical transition? Two candidates in the literature are infinitely thin hard rods on a lattice[65] and a space filling self-avoiding chain on a lattice.[66] We leave further exploration for the future.

But the issue of *apparent transitions* does already arise in the simple KA models. As mentioned at the end of Section 4 dramatic slowing down in finite dimensions can occur near an almost sharp *avoided transition* associated with a crossover from non-cooperative to cooperative dynamics. In particular, some high dimensional lattices – including already some three dimensional lattices – are approximately tree-like out to some number of neighbors; if the dimension increases while the coordination number remains fixed, such tree-like local structure suggests that a ghost of the Bethe lattice transition with the same local structure will become more and more apparent. More generally, it is likely that in the limit of high dimensions, models that have low-dimensional frozen structures – such as $s = d - 1$ on hypercubic lattices which has frozen one-dimensional bars – will, as the density increases, have increasingly rapid crossovers that appear more and more like an actual transition.

In this paper, we have studied Bethe lattices with loops that interpolate between the finite dimensional lattice and the standard Bethe lattice. In this case, there is always a transition although it is pushed to a density that approaches one when the finite-dimensional regions become large. From the other direction, it would be interesting to analyze a Kac-like interpolation for a fixed finite dimensional lattice with longer and longer

range connections which converges in a certain limit to a Bethe lattice. In this case, the transition will presumably never occur, but the cross-over will become sharper and sharper near the critical density on the Bethe lattice.

7.2. Comparison with Mean-field Approaches

We have found that the generic behavior of KA models on Bethe lattices (exceptions being $s = k - 1$), has a transition with features similar to both first order and critical transitions. Although the density of frozen particles jumps discontinuously at the critical density, there are precursor effects as the transition is approached from the frozen phase and, at least for some quantities, also from the ergodic phase. In particular, we have seen that divergence of characteristic length and time scales is apparent in the dynamic density–density correlations and the related dynamical susceptibility.

This mixed behavior, as well as several more specific features, is similar to that found in certain mean-field-like theoretical analyses conjectured to be relevant for glass transitions. In particular, spin models with *quenched random* interactions that couple collections of $p > 2$ spins have been studied.[32, 67] It turns out that the infinite-range versions of such random p-spin models have a real thermodynamic transition at a critical temperature, however interesting dynamical behavior commences sharply at a higher temperature, T_D, without singularities in static properties. This is interpreted as the onset of ergodicity breaking: below T_D the equilibrium measure is fractured in exponentially many metastable "states" ("TAP" states which are locally stable solutions of the self-consistent mean-field equations); the large number of these give rise to a configurational entropy density, S_c, that jumps to a non-zero value at T_D. As the temperature is lowered further, S_c decreases, vanishing at the thermodynamic transition. Due to the presence of quenched random disorder p-spin models would seem to have little to do with glasses which must generate their own randomness, but it has been shown that some mean-field approximations to non-random models, in particular the mode-coupling approximation,[31] give rise to self-consistent integral equations with very similar structure to the one of this models.[32] In particular, mode coupling equations give rise to an analogous ergodicity-breaking transition at a finite. We find that the same properties are shared by KA models on Bethe lattices, for which at a finite critical density the configuration space is broken into many ergodic components and the configurational entropy jumps to a non-zero value and then decreases at higher densities (here the thermodynamics is trivial and, hence, S_C equals zero only at unit density). In addition, the auto-correlation function, $C(t)$, and the associated susceptibility, $\chi_4(t)$, which

we computed numerically for Bethe lattices with $k = 3$, $s = 1$, behave similarly to those found for the infinite range random p-spin models and in the Mode Coupling Theory.[59,68,69] Indeed, even the off-equilibrium aging behavior of KCM on Bethe lattices is quite similar to the one obtained for mean-field quenched random systems.[64]

While tempting to conclude that these behaviors are all manifestations of the same physical phenomena, one must be careful. In particular the dynamical transition in KA models on Bethe lattices is a reducible/irreducible transition whereas for p-spin models the irreducibility is guaranteed and the breaking of the ergodicity is due to the thermodynamic limit (i.e. p-spin models are irreducible and hence ergodic on finite volume, however an ergodicity-breaking transition occurs in infinite volume due to the existence of a thermodynamic transition). Nevertheless, to explore whether, and in what sense, some of the mean-field approximations might capture some of the essential physics of more realistic finite dimensional models, the possible connections to the KA models are worth exploring further.

7.3. Experimental Issues and Prospects

Kinetically constrained lattice gas models, while they may capture some of the important features of glass transitions – or almost transitions – clearly have major flaws. First, in any real system, rates of local processes cannot strictly vanish. Thus there will also be some constraint-violating processes. Second, while lattice models are often good approximations for static properties, for dynamics of systems in which the geometry and/or bonding is believed to play an important role, it is dangerous to appeal to universality arguments for the validity of lattice models. This is especially true if the length scales of the important processes never get very large, as is believed to be the case for glasses.[3]

Both of these issues merit much further attention. In particular, one should at a minimum consider the effects of a low rate of constraint-violating particle motions within the lattice model framework. In practice, the neglect of certain processes may be a good approximation on a wide range of time scales. For example, if there are chemical bonds with energies much larger than $k_B T$, then the ratio of the rates of processes between, e.g., those that require breaking of two bonds and those that require breaking three or more, may be very small. A – and arguably *the* – fundamental problem of dynamics near glass transitions is the large and rapidly onsetting increases in the effective activation barriers. Thus, looking for an explanation that involves a rapid crossover from domination by a relatively fast process to freezing out of this and the ensuing domination of relaxation by a much slower process, is surely a productive direction.

The issue of continuum versus lattice models is a trickier one. If geometrical constraints really dominate near glass transitions, then one needs to consider how to model the interplay between energetic and entropic barriers, even if the former only arise from repulsive interactions that are not entirely hard-core. In principle, from simulations or from computations of more realistic continuum models of molecular interactions, one may be able to extract effective rates for various local processes (see ref. 12 for an investigation in this direction). If temperature changes dominate over density changes[70] the effective density parameter in a lattice approximation will not be simply related to the actual density because of soft-core effects. Nevertheless, if free-volume ideas of glass transitions are relevant, one should be able to work in terms of some effective density – with "vacancies", or at least mobile ones, representing the free volume. Because of local expansion and contraction, however, the free volume is in general not conserved. One might expect the particle conservation to play a crucial role in KA models. In fact, this is not the case, as the non-conserving FA model shows very similar behavior to KA models. Presumably, a better approximation would conserve (effective) density most of the time, but not always.

We leave these issues and any attempts at direct comparisons with experiments, for future papers.

8. ACKNOWLEDGMENTS

REFERENCES

1. See e.g. P. G. Debenedetti and F. H. Stillinger, *Nature* **410**:259 (2001).
2. P. G. De Benedetti, *Metastable Liquids* (Princeton University Press, 1997).
3. Ediger, *Annu. Rev. Phys. Chem.* **51**:99 (2000).
4. E. R. Weeks, J. C. Crocker, A. C. Levitt, A. Schofield, and D. A. Weitz, *Science* **287**:627 (2000).
5. M. M. Hurley, and P. Harrowell, *Phys. Rev. E* **52**:1694 (1995) and refs. therein.
6. R. Yamamoto and A. Onuki, *Phys. Rev. Lett.* **81**:4915 (1998) and refs. therein.
7. C. Bennemann, C. Donati, J. Bashnagel, and S. C. Glotzer, *Nature* **399**:246 (1999); S. C. Glotzer, V. V. Novikov, and T. B. Schroeder, *J. Chem. Phys.* **112**:509 (2000); N. Lacevic, F. W. Starr, T. B. Schroeder, and S. C. Glotzer, *J. Chem. Phys.* **119**:7372 (2003) and refs. therein.
8. L. Berthier, *Phys. Rev. E* **69**:020201(R) (2004).

9. F. Ritort and P. Sollich, *Adv. Phys.* **52**:219 (2003).

10. J. Jackle, *J. Phys. Condens. Matter* **14**:1423 (2002).

11. W. Kob and H. C. Andersen, *Phys. Rev. E* **48**:4364 (1993).

12. J. P. Garrahan and D. Chandler, *PNAS* **100**:9710 (2003); J. P. Garrahan and D. Chandler, *Phys. Rev. Lett.* **89**:035704 (2002).

13. G. Biroli and M. Mézard, *Phys. Rev. Lett.* **88**:025501 (2002); O. Rivoire, G. Biroli, O. C. Martin, and M. Mézard, *Eur. Phys. J. B* **37**:55 (2004).

14. E. Marinari, and E. Pitard, *A Topographic-Non-Topographic Paradigm for Glassy Dynamics*, cond-mat/0404214.

15. D. R. Reichman, E. Rabani, and P. L. Geissler, *Comparison of Dynamical Heterogeneity in Hard-Sphere and Attractive Glass Formers*, cond-mat/0406136. P. L. Geissler, D. R. Reichman, *Short-ranged attractions in jammed liquids: How cooling can melt a glass*, cond-mat/0402673.

16. C. Chamon, P. Charbonneau, L. F. Cugliandolo, D. R. Reichman, and M. Sellitto, *Out-of-equilibrium dynamical fluctuations in glassy systems*, cond-mat/0401326.

17. L. Berthier and J. P. Garrahan, *Phys. Rev. E* **68**:041201 (2003); L. Berthier and J. P. Garrahan, *J. Chem. Phys.* **199**:4367 (2003).

18. A. Lawlor, D. Reagan, G. D. McCullagh, P. DeGregorio, P. Tartaglia, and K. A. Dawson, *Phys. Rev. Lett.* **89**:245503 (2002).

19. S. Whitelam, L. Berthier, and J. P. Garrahan, *Phys. Rev. Lett.* **92**:185705 (2004).

20. S. Franz, R. Mulet, and G. Parisi, *Phys. Rev. E* **65**:021506 (2002).

21. J. Kurchan, L. Peliti, and M. Sellitto: *Europhys. Lett.* **39**:365–370 (1997).

22. A. Barrat, J. Kurchan, V. Loreto, and M. Sellitto,. *Phys. Rev. Lett.* **85**:5034–5038 (2000).

23. J. Kurchan, Proceedings in ref. 28.

24. L. Berthier, *Phys. Rev. Lett.* **91**:055701 (2003).

25. Y. J. Jung, J. P. Garrahan, and D. Chandler, *Phys. Rev. E* **69**:061205 (2004); L. Berthier, D. Chandler, and J. P. Garrahan, *Length scale for the onset of Fickian diffusion in supercooled liquids* cond-mat/0409428; A. C. Pan, J. P. Garrahan, and D. Chandler, *Heterogeneity, growing lengthscales, and universality in the dynamics of kinetically constrained lattice gases in two dimensions*, cond-mat/0410525.

26. M. Sellitto, and J-J. Arenzon, *Phys. Rev. E* **62**:(2000) 7793.

27. H. M. Jaeger, J. B. Knight, and R. P. Behringer, *Rev. Mod. Phys.* **68**:1259–1273 (1996).

28. A.-J. Liu, and S.-R. Nagel (ed.) *Jamming and Rheology: Constrained Dynamics on Microscopic and Macroscopic Scales* (Taylor and Francis, London, 2001).

29. G. H. Fredrickson and H. C. Andersen, *Phys. Rev. Lett.* **53**:1244 (1984); *J. Chem. Phys.* **83**:5822 (1985); G. H. Fredrickson and S. A. Brawer, *J. Chem. Phys.* **84**:3351 (1986).

30. T. M. Liggett, *Interacting Particle Systems* (Springer-Verlag, New York, 1985).

31. W. Gotze in *Liquids Freezing and the Glass Transition*, Hansen J.P., Levesque D., and J. Zinn-Justin ed. (North-Holland Amsterdam, 1991), pp. 287–503.

32. J. P. Bouchaud, L. F. Cugliandolo, J. Kurchan, and M. Mézard, *Spin Glasses and Random Fields*, Singapore 1998. World Scientific. L. F. Cugliandolo, Les Houches Session 77 July 2002 J-L. Barrat, J. Dalibard, J. Kurchan, M. V. Feigel'man eds.

33. C. Kipnis, and S. R. S. Varadhan, *Comm. Math. Phys.* **104**:1–19 (1986).

34. H. Spohn, *Large Scale Dynamics of Interacting Particles* (Berlin, Springer, 1991).

35. H. Spohn *J. Stat. Phys.* **59**:1227–1239 (1990).

36. P. Harrowell, *Phys. Rev. E* **48**:4359 (1993).

37. R. Kohlrausch, *Ann. Phys.* **12**:393 (1847).

38. G. Williams, and D. C. Watts, *Trans. Faraday Soc.* **66**:80 (1980).

39. D. A. Huse and D. S. Fisher, *Phys. Rev. B* **35**:6841 (1987).

40. C. Toninelli, G. Biroli, and D. S. Fisher, *Phys. Rev. Lett.* **92**:185504 (2004).

41. C. Toninelli and G. Biroli, *J. Stat. Phys.* **117**:27 (2004).
42. M. D. Ediger, How molecules move near the glass transition temperature, Invited talk at the APS March meeting.
43. R. Cerf, and F. Manzo, *Stoch. Proc. Appl.* **101**:69 (2002).
44. J. Reiter, *J. Chem. Phys.* **95**:544 (1991).
45. A. C. D. van Enter, J. Adler, and J. A. M. S. Duarte, *J. Stat. Phys.* **60**:323 (1990).
46. L. Bertini, and C. Toninelli, in *Exclusion processes with degenerate rates: convergence to equilibrium and tagged particle,* cond-mat/0304694, accepted by *J. Stat. Phys.*
47. B. DeFinetti, *Atti R. Acc. Naz. Lincei serie* 6 **4**:251 (1931).
48. H.-O. Georgii, *Lecture Notes in Mathematics* Vol. **760** (Springer, Berlin, 1979).
49. J. Adler, *Physica A* **171**:435 (1991).
50. J. Chalupa, P. L. Leath, and G. R. Reich, *J. Phys. C* **12**:L31 (1979).
51. M. Aizenmann and J. L. Lebowitz, *J. Phys. A* **21**:3801 (1988).
52. A. E. Holroyd, *Probab. Theory Rel* **125**:195 (2003).
53. C. Toninelli, G. Biroli, and D. S. Fisher, in preparation.
54. P. De Gregorio, A. Lawlor, P. Bradley, and K. A. Dawson, *Phys. Rev. Lett.* **93**:025501 (2004).
55. L. Chayes, V. J. Emery, S. A. Kivelson, Z. Nussinov, and J. Tarjus, *Physica A* **225**:129 (1996).
56. N. C. Wormald, *Models of Random Regular Graphs* in *Surveys in Combinatorics*, Lamb, J. D. and Preece, D. A. eds. London Mathematical Society Lecture Note Series Vol. **216** (Cambridge University Press, UK, 1999), p. 239.
57. M. E. Fisher and J. W. Essam, *J. Math. Phys.* **2**:609 (1961).
58. M. Aizenman, J. T. Chayes, L. Chayes, and C. M. Newman, *J. Stat. Phys.* **50**:1 (1988).
59. S. Franz, and G. Parisi, *J. Phys.: Condens. Matter* **12**:6335 (2000);C. Donati, S. Franz, G. Parisi, and S. C. Glotzer, *J. Non-Cryst. Solids* **307–310**:215 (2002).
60. M. Pretti, *J. Stat.Phys.* **111**:993 (2003).
61. R. H. Schonmann, *Ann. Probab.* **20**:174 (1992).
62. R. Cerf, E. Cirillo, *Ann. Probab.* **27**(4):1837 (1999).
63. S. J. Pitts, T. Young, and H. C. Andersen, *J. Chem. Phys.* **113**:8671 (2000); J. Reiter, F. Mauch, and J. Jackle, *Physica A* **184**:458 (1992).
64. M. Sellitto, G. Biroli, and C. Toninelli, *Facilitated spin models on Bethe lattice: bootstrap percolation, mode-coupling transition and glassy dynamics*, cond-mat/0409393.
65. R. Renner, H. Lowen, and J.-L. Barrat, *Phys. Rev. E* **52**:5091 (1995); S. Obukhov, D. Kobsev, D. Perchak, and M. Rubinstein, *J. Phys. I France* **7**:563 (1997).
66. R. Du, A. Grosberg, T. Tanaka, and M. Rubinstein, *Phys. Rev. Lett.* **84**:2417 (2000).
67. L.-F. Cugliandolo, and J. Kurchan, *Phys. Rev. Lett.* **71**:173–176 (1993).
68. T. R. Kirkpatrick, and D. Thirumalai, *Phys. Rev. A* **37**:4439 (1988).
69. G. Biroli and J.-P. Bouchaud, *Europhys. Lett.* **67**:21 (2004).
70. G. Tarjus, D. Kivelson, S. Mossa, and C. Alba-Simionesco, *Disentangling density and temperature effects in the viscous slowing down of glassforming liquids*, cond-mat/0309579.